BAMS Article

The Bolzano Tracer Experiment (BTEX)

Dino Zardi, Marco Falocchi, Lorenzo Giovannini, Werner Tirler, Elena Tomasi, Gianluca Antonacci, Enrico Ferrero, Stefano Alessandrini, Pedro A. Jimenez, Branko Kosovic, and Luca Delle Monache

ABSTRACT: The paper describes the observational and modeling efforts performed under the Bolzano Tracer Experiment (BTEX). BTEX focused on the basin surrounding the city of Bolzano, at the junction of three tributary valleys on the southern side of the Alps, to characterize the ground-level impact of pollutants emitted by a waste incinerator close to the city, and atmospheric factors controlling dispersion processes in the whole basin, under different winter weather situations. As part of the experiment, two controlled releases of a passive gas tracer (sulfur hexafluoride, SF_6) were performed through the stack of the incinerator on 14 February 2017 at two different times, starting respectively at 0700 and 1245 LST, representative of distinct phases of the daily cycle. Samples of ambient air were collected at target sites, and later analyzed using a mass spectrometer, allowing a detectability limit down to 30 ppt. Meanwhile, meteorological conditions were continuously monitored by means of a high-resolution, nonconventional network of ground-based instruments, including 15 weather stations, one temperature profiler, one sodar, and one Doppler wind lidar. Data from the above measurements represent one of the rare examples of integrated datasets available to the community for the characterization of dispersion processes in a typical mountainous environment. In particular, they offered a reference benchmark for testing and calibrating a series of combined numerical modeling suites for weather prediction and pollutant dispersion simulation in such a complex terrain, as shown in the paper.

KEYWORDS: Complex terrain; Mesoscale processes; Dispersion; Lidars/Lidar observations; Tracers; Air pollution

https://doi.org/10.1175/BAMS-D-19-0024.1
Corresponding author: Prof. Dino Zardi, dino.zardi@unitn.it
In final form 6 November 2020

AFFILIATIONS: Zardi—Atmospheric Physics Group, Department of Civil Environmental and Mechanical Engineering, and Center Agriculture Food Environment, University of Trento, Trento, Italy; **Giovannini**—Atmospheric Physics Group, Department of Civil Environmental and Mechanical Engineering, University of Trento, Trento, Italy; **Tirler**—Eco-Research s.r.l., Bolzano, Italy; **Falocchi, Tomasi, and Antonacci**—CISMA s.r.l., Bolzano, Italy; **Ferrero**—University of Eastern Piedmont, Alessandria, Italy; **Alessandrini, Jimenez, and Kosovic**—National Center for Atmospheric Research, Boulder, Colorado; **Delle Monache**—National Center for Atmospheric Research, Boulder, Colorado, and Center for Western Weather and Water Extremes, Scripps Institution of Oceanography, University of California, San Diego, La Jolla, California

Atmospheric processes occurring over complex terrain—e.g., hills, mountains, valleys, or basins—are characterized by inherently intricate flows (Whiteman 2000). These originate from a variety of landforms, as well as from contrasts among diverse land use and land cover—such as in natural/rural versus densely urbanized areas (Giovannini et al. 2014b)—which add up to the many different mechanisms making exchange and transport processes in the atmospheric boundary layer intrinsically complex (Serafin et al. 2018).

Among these processes, those governing the dispersion of pollutants in complex terrain still pose many challenging open questions, not only for the intrinsic limitations of the available observational and modeling tools, but also for the lack of appropriate conceptual schemes and theoretical background (Giovannini et al. 2020).

In particular, among the variety of complex Earth's landforms, valleys and basins display peculiar properties. Here ventilation from upper winds is significantly reduced, as the sidewalls shelter the lowest layers, below the crest levels, from downward penetration of upper flows, especially in deeper valleys and basins. In addition, nighttime radiative cooling favors the pooling of deep cold layers in the lowlands, and further surface cooling at the valleys' and basins' floors is enhanced by the convergence of drainage flows along the sidewalls. These situations typically produce strongly stratified, stable layers that suppress turbulent mixing and, further, inhibit the penetration of upper flows down to the lower levels. In particular, recurrent stagnation situations (e.g., cold pools) may occur in depressed or confined areas, especially during wintertime (Conangla et al. 2018).

On the other hand, when there is no upper forcing—such as under well-leveled, large-scale, high pressure fields, typically associated with anticyclonic situations and clear skies—the diurnal cycle of strong incoming solar radiation during daytime, and longwave outgoing radiation at nighttime, promotes the development of organized daily periodic thermally driven winds (Zardi and Whiteman 2013). These winds typically are directed up-slope during daytime and downslope during nighttime, and are associated with peculiar turbulence structures (Rotach and Zardi 2007). The extent and strength of these circulations is strongly dependent upon a series of factors, including the overall synoptic-scale situation, as well as weather conditions during the preceding days. For instance, after rainy days, increased soil moisture is typically associated with larger latent heat fluxes, reducing the available sensible heat fluxes required for raising surface air temperatures, and forcing the above flows.

The detailed representation of the above-described flows—which is required for a series of operational applications, including air quality management—still poses serious challenges, both to observing systems and to numerical models (cf. Serafin et al. 2018 for a thorough review).

Indeed, the need for understanding the nature and characteristics of transport processes over complex terrain has continuously stimulated various research projects. In the past, the research project Atmospheric Studies in Complex Terrain (ASCOT) conducted an intensive

field study in the Brush Creek Valley of western Colorado in September–October 1984 (Clements et al. 1989). The overall objective of the study was to enhance the understanding of pollutant transport and diffusion associated with valley flows. Data collections were designed to investigate nocturnal and morning transition of wind, turbulence, and temperature fields in the valley, its tributaries, and on its sidewalls. Accordingly, targeted release and sampling of atmospheric tracers were also used to study transport and diffusion (Orgill 1989; Allwine 1993).

Furthermore, under the umbrella of the Mesoscale Alpine Programme (MAP), the MAP-Riviera project offered in 1999 the opportunity for an unprecedented deployment of many different observational resources, including airborne measurements and tracer releases, for an in-depth investigation of turbulence and boundary layer processes in the Riviera Valley in Switzerland (Rotach et al. 2004a).

More recently, the project Alpine Noise and Air Pollution Study (ALPNAP) investigated the effects of local atmospheric processes controlling propagation of acoustic noise and dispersion of air pollution, originating from traffic, along two major routes in the Alps, i.e., the Brenner and Frejus corridors (de Franceschi and Zardi 2009; Gohm et al. 2009; Schicker and Seibert 2009; Trini Castelli et al. 2011).

The project Vertical Transport and Mixing (VTMX) performed in 2000 in the Salt Lake Valley (Doran et al. 2002) investigated the vertical transport and mixing in the boundary layer, particularly under stably stratified conditions, and weak or intermittent turbulence, during the morning/evening transitions. The project concentrated in urban basins or valleys, and on phenomena such as formation and evolution of inversions and transport of pollutants around layers trapped in valleys. Similarly, the project Persistent Cold-Air Pool (PCAPS) explored extensively in 2010–11 the persistence of long-lasting cold pools in the Salt Lake Valley and its implications for air quality (Lareau et al. 2013). Also, the project Mountain Terrain Atmospheric Modeling and Observations (MATERHORN) investigated complex-terrain meteorology over a wide range of scales, topographic features, and driving mechanisms by drawing expertise from multiple disciplines and by employing complementary research methodologies (Fernando et al. 2015). Two major field experiments were conducted in fall 2012 and spring 2013 at the Granite Mountain Atmospheric Sciences Testbed (GMAST) of the U.S. Army Dugway Proving Ground (DPG) in Utah, collecting high-resolution measurements focusing on conditions dominated by either thermally driven circulations or strong synoptic forcing. More recently, the project Passy-2015 (Paci et al. 2016) concentrated on atmospheric dynamics and air quality in the Arve River Valley near the city of Passy in the French Alps, combining field measurements and high-resolution modeling of pollutant transport under unfavorable conditions (Sabatier et al. 2020a,b), especially connected to persistent inversions and cold air pool situations in the area and its surroundings (Largeron and Staquet 2016a,b; Arduini et al. 2016, 2020; Quimbayo-Duarte et al. 2019a,b).

Finally, the ongoing cooperative research program Multi-scale transport and exchange processes in the atmosphere over mountains – programme and experiment (TEAMx) is pursuing the goal of exploring further transport and exchange processes characterizing mountainous areas at different scales, through a combined approach including both intensive field measurements, by means of integrated instrumental systems and platforms concentrated at selected target areas, and high-resolution numerical modeling (Serafin et al. 2018, 2020).

To trace precisely the processes controlling the dispersion of pollutants, a number of research projects included controlled releases of tracers as part of their field campaigns: a comprehensive summary is offered in Table 1. By means of these experiments, different situations have been explored, ranging from ground-level emissions to elevated sources (e.g., stacks of industrial plants). In particular, the European Tracer Experiment (ETEX: Van dop et al. 1998; Nodop et al. 1998) focused on the comparative assessment of the ability of various dispersion

Table 1. Summary of research projects on pollutant dispersion including controlled releases of tracers as part of their field campaigns (country abbreviations are U.S. = United States, NL = Netherlands, DK = Denmark, U.K. = United Kingdom, ES = Spain, CH = China, DE = Germany, FR = France, and CA = Canada).

Years	Experiment	Site	Country	Tracer	Source elevation		Terrain		Environment			References
					Surface	Elevated	Simple	Complex	Rural	Urban	Mountain	
1954–55, 1957	Round Hill	Boston	U.S.	SO_2	X		X		X			Cramer et al. (1958)
1956	Project Prairie Grass	O'Neil	U.S.	SO_2	X		X		X			Barad (1958) and Haugen (1959)
1959	Green Glow	Hanford	U.S.	ZnS	X		X		X			Fuquay et al. (1964) and Nickola (1977)
1960–61	Hanford-30	Hanford	U.S.	ZnS	X		X		X			Fuquay et al. (1964) and Nickola (1977)
1961–62	Dry Gulch	Vandenberg	U.S.	ZnS	X		X		X			Haugen and Fuquay (1963)
1961–62	Ocean Breeze	Cape Canaveral	U.S.	ZnS	X		X		X			Haugen and Fuquay (1963)
1963–73	Hanford-67	Hanford	U.S.	ZnS	X	X	X		X			Nickola (1977)
1964	Hanford-64	Hanford	U.S.	ZnS		X	X		X			Nickola et al. (1983)
1975–77	SRPTEX	Aiken	U.S.	Kr-85		X	X		X			Telegadas et al. (1980)
1977–78	Cabauw	Cabauw	NL	SF_6		X	X		X			Nieuwstadt and van Duuren (1979)
1978–79	Copenhagen	Copenhagen	DK	SF_6		X		X		X		Gryning and Lyck (1980, 1984, 2002)
1978–79	—	Southern Weald	U.K.	SF_6		X		X			X	Emberlin (1981)
1980	OKTEX	Norman	U.S.	PTCH, PMCH, SF_6	X		X		X			Ferber et al. (1981) and Moran and Pielke (1989a,b)
1980	ASCOT	California	U.S.	SF_6	X	X		X			X	Dickerson and Gudiksen (1983), Clements et al. (1989), Orgill (1989), Whiteman (1989), Gudiksen and Shearer (1989), and Allwine (1993)
1980–81	Kincaid	Kincaid	U.S.	SF_6		X	X		X			Bowne et al. (1983)
1982	Bull Run	Claxton	U.S.	SF_6		X	X		X			Bowne et al. (1983)
1982–83	ACURATE	Aiken	U.S.	Kr-85		X	X		X			Heffter et al. (1984)
1983	CAPTEX	Dayton, Sudbury	U.S.	PMCH		X	X					Ferber et al. (1986), Haagenson et al. (1987), and Hegarty et al. (2013)
1983	Hanford-83	Hanford	U.S.	SF_6	X		X		X			Doran and Horst (1985)
1984	METREX	Washington D.C., Rockville, and Lorton	U.S.	PMCH, PDCH	X			X		X		Draxler (1985)
1985	Teruel	Teruel	ES	SF_6	X		X		X			Sivertsen and Irwin (1987, 1996) and Sivertsen (1988)
1985	Indianapolis	Indianapolis	U.S.	SF_6	X			X		X		Murray and Bowne (1988)
1985	SCCCAMP	Santa Barbara, CA	U.S.	PFMCP	X			X		X		Pennell et al. (1987) and Strimaitis et al. (1991)
1986–87	—	Los Alamos	U.S.	Radionuclides			X	X	X			Bowen (1994)
1987	—	Mogollon Rim, Arizona	U.S.	SF_6	X			X			X	Bruintjes et al. (1995)
1987	ANATEX	Glasgow, St. Cloud	U.S.	PTCH	X		X		X			Draxler and Heffter (1989), Haagenson et al. (1990), and Sykes et al. (1993)

Table 1. (Continued).

Years	Experiment	Site	Country	Tracer	Source elevation		Terrain		Environment			References
					Surface	Elevated	Simple	Complex	Rural	Urban	Mountain	
1989–91	TRANSALP 90	Canton Ticino	CH	C7F14	X			X			X	Ambrosetti et al. (1994, 1998)
1989	IACP	Roanoke, VA	U.S.	SF_6	X			X			X	Allwine et al. (1992)
1990	1990 NGS Visibility Study	Grand Canyon	U.S.	PFC	X			X			X	Chen et al. (1999)
1991	LMOS—Lake Michigan Ozone Study	Lake Michigan	U.S.	SF_6	X		X			X		Wilkerson (1991) and Eastman et al. (1995)
1992	TRACT	Sasbach	DE	PDCH-C_8F_{16}	X			X			X	Zimmerman (1995)
1992	MOHAVE	Grand Canyon	U.S.	oPDCH	X			X			X	Pitchford et al. (1997), Green (1999), and Koračin et al. (2000)
1994	ETEX	(FR-E)	FR	PMCH, PMCP		X			X	X		Van dop et al. (1998) and Nodop et al. (1998)
1996	SLOPE	Freiburg-Schauinsland	DE	SF_6	X			X			X	Fiedler et al. (2000) and Kalthoff et al. (2000)
1997	Model Validation Program experiments	Vandenberg Air Force Base	U.S.	SF_6								Min et al. (2002)
1999	MAP	Riviera Valley	CH	PFC	X			X			X	Rotach et al. (2004a)
1999–2000	URGENT/PUMA	Birmingham	U.K.	PMCH	X		X			X		Britter et al. (2002)
2000	VTMX	Salt Lake Valley	U.S.	PFC	X							Doran et al. (2002) and Fast et al. (2006)
2000	URBAN 2000	Salt Lake City	U.S.	SF_6	X	X		X		X		Allwine et al. (2002)
2001	—	Ellerslie, Alberta	CA	CH_4	X			X	X			Flesch et al. (2004)
2002	—	Vandenberg	U.S.	SF_6		X	X					Min et al. (2002)
2002	BUBBLE	Basel	CH	SF_6	X			X		X		Rotach et al. (2004b)
2003	JU2003	Oklahoma City	U.S.	SF_6	X			X		X		Allwine et al. (2004), Clawson et al. (2005), Allwine and Flaherty (2006), Doran et al. (2007), and Flaherty et al. (2007)
2003–04	DAPPLE	London	U.K.	PMCH	X			X		X		Martin et al. (2010a,b) and Wood et al. (2009)
2010–12	FluxSAP	Nantes	FR	SF_6	X			X		X		Mestayer et al. (2011) and Connan et al. (2015)

models in simulating emergency response situations in various different countries in northern Europe. Here releases of passive tracers, both from elevated sources and from surface level, were carried out to identify how pollutants migrate within the urban environment.

These concentration datasets, once shared within the community, provided very important common reference benchmarks for testing developments and improvements in dispersion models, even long after the experiments were performed (cf. Ngan et al. 2015; Ngan and Stein 2017).

However, Table 1 shows that only few of the above projects were conducted over complex mountainous terrain. This is very likely due to the intrinsic difficulties in designing and managing measurement campaigns in such a challenging environment. Nevertheless, significant efforts were made in recent years to improve our modeling capabilities, and datasets for verification of progress made with numerical simulations would be highly valuable (e.g., Giovannini et al. 2014a,b, 2017, 2020; Tomasi et al. 2017, 2019; Serafin et al. 2018; De Wekker et al. 2018).

Accordingly, the present paper contributes to filling this gap by providing an overview of the scope, concept, implementation and results of the Bolzano Tracer Experiment (BTEX). Indeed, the project aimed at performing a careful environmental impact assessment of the fate of emissions from a waste incinerator south of the city of Bolzano in the Italian Alps. In view of that, it also offered the opportunity to investigate in depth the complex atmospheric processes occurring in the surrounding area, that were only partly envisaged by previous studies (cf. Dosio et al. 2001; Laiti et al. 2013a,b, 2014). To take appropriately into account these processes, a remarkable part of the effort was invested in setting up and testing different combinations of numerical weather prediction and pollutant dispersion models, in order to simulate as precisely as possible the transport and diffusion of emissions from the incinerator under various situations. In particular, the testing phase aimed at evaluating the model performance for both short- and long-term prediction of the dispersion of pollutants emitted by the plant. To accomplish this goal, a suitable observational basis of passive tracer concentrations from controlled releases through the chimney of the incinerator was collected, as part of a field campaign also including an intensive deployment of various instruments for meteorological measurements in the area. The series of results obtained from the project turned out to be applicable well beyond the present case study: indeed, Bolzano is a medium-sized city located in a rather wide basin, so understanding phenomena occurring in Bolzano basin may cast new light on many other quite similar situations, not only in the Alps, but also in many other comparable mountain range systems. Accordingly, the present paper was also motivated by the will of disseminating these results among a broader community.

The paper is organized as follows: the target area and the waste incinerator layout are introduced, the concept and design of the BTEX project are outlined, the modeling chains adopted for simulations are presented, and their results are discussed. Finally, some conclusions and an outlook for future research are drawn.

Outline of the situation

Characterization of the target area. Bolzano (in German *Bozen*) is a mid-size city in the central Italian Alps, and the most populated urban area (about 108,000 inhabitants as of 2019) in South Tyrol. Here people speak either German or Italian (hence names in German will be added in parentheses in italics).

The city expands in a wide open and flat area of the Adige Valley (*Etschtal*) at 262 m MSL, where the Talvera (*Talfer*) River and the Isarco (*Eisack*) River join the Adige (*Etsch*) River. Here, the Adige Valley bends from east–west to north–south oriented, and two tributary valleys, where the above rivers flow—namely, the Sarentina Valley (*Sarntal*) and the Isarco Valley (*Eisacktal*)—join from the north and the east, respectively (Fig. 1). These valleys are rather deep, as their steep sidewalls are rather uniformly flanking them, and their crests easily exceed 1,200 m MSL. In particular, the Adige Valley is a typical U-shaped glacial valley, with a quite wide floor, whereas the Sarentina Valley and the Isarco Valley are rather V-shaped. The climate of Bolzano is continental, characterized by warm summers and cold winters. Wind regimes are dominated by terrain effects (Dosio et al. 2001). Occasionally, pressure gradients across the Alps may result in moderate to strong dynamically driven orographic winds (föhn). Instead, in the absence of significant synoptic-scale forcing, the local wind regime is dominated by the

daily periodic development of thermally driven winds (Giovannini et al. 2015, 2017). In particular, during daytime the wind blows up-valley in the Adige Valley and interacts with those developing into the Sarentina Valley and into the Isarco Valley. During nighttime downslope drainage flows develop along the sidewalls and feed down-valley winds, which merge at the confluence of the tributary valleys. The valley topography controls the penetration of solar radiation (cf. Laiti et al. 2018) as well as the outgoing longwave emission, and hence the heat budgets affecting the thermal structure of the lower atmosphere. As a consequence, local winds are mostly absent or very weak during wintertime (de Franceschi et al. 2009; Falocchi et al. 2019, 2021), whereas ground-based thermal inversions often occur at the valley floors during nighttime. The combination of these factors determines frequent and persistent stagnation conditions, which are very critical for air quality in the area: Fig. 2 provides an overview of the occurrence of different stability situations in wintertime in the area.

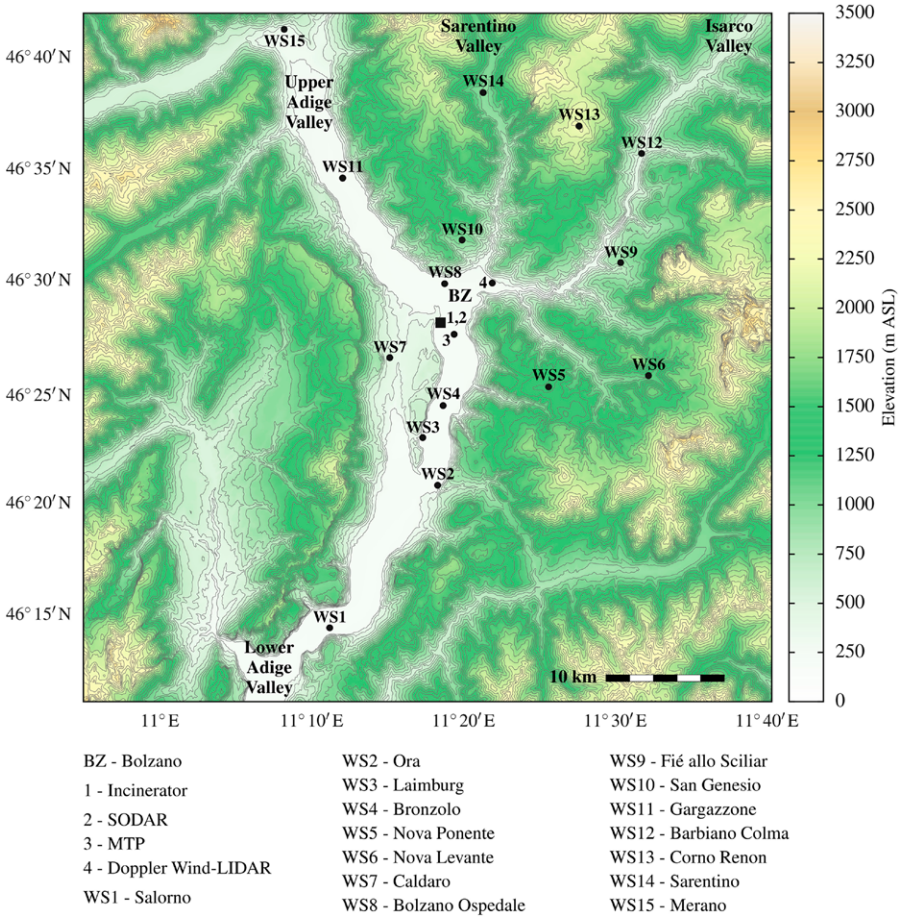

Fig. 1. Overview of the BTEX target area and surrounding mountains and valleys around the city of Bolzano (BZ): the map indicates the incinerator (labeled 1), and the monitoring systems used during BTEX, including one sodar (labeled 2), one microwave temperature profiler (labeled 3), one Doppler wind lidar (labeled 4), and 15 ground-based weather stations (WS1–WS15) (reproduced with permission from Falocchi at al. 2020).

A peculiar feature was observed at the narrow outlet of the Isarco Valley: here the drainage wind often accelerates and spreads into the Bolzano basin in the form of a valley exit jet (see sidebar), with peaks of wind strength exceeding 12 m s^{-1} (Tomasi et al. 2019; Falocchi et al. 2020).

Under such varied situations, pollutant transport processes may display quite nontrivial patterns. A similar example is reported in Hanna et al. (1984) for a case study at the Westvaco Luke Mill in western Maryland (United States): a scenario with a deep river valley, up- and down-valley flows depending on time of day, and plume impaction on nearby hillsides.

Characterization of the emissions. The waste incinerator is about 2 km southwest of Bolzano, in the lower Adige Valley (black square in Fig. 1). The plant started operating in July 2013, with a maximum waste treatment capacity of 130,000 t yr^{-1}. The post-combustion treatment of the exhaust smokes includes a system for the abatement of pollutants and a series of probes monitoring their physical properties and chemical composition, before release into the atmosphere through a chimney 60 m high AGL. Under usual operating conditions, they are ejected at a constant flow rate of 105 Nm^3 h^{-1} with a temperature of 413 K. Therefore, the

impact areas of the pollutants and their ground concentrations mostly depend on local atmospheric processes, in particular wind regime and stability, as well as on the effective source height (see section "Ex-post simulations" below).

The city of Bolzano, as well as the surrounding suburban areas, are rather densely populated (2,060 inhabitants per square kilometer), and major infrastructure—including many roads, a major highway, many factories, and industrial plants—concentrates there. As a consequence, various sources of air pollutants exist in the area, as shown by the Emission Inventory provided by the Environmental Agency of the Autonomous Province of Bolzano (Fig. 3). Among them, domestic heating and local traffic play a major role. In particular, the Brenner Highway crosses the whole basin, north to south, through the middle of the urban area. With its annual flow of about 16 million vehicles, including both cars and heavy lorries (trucks), it is a major source of nitrogen oxides (NO_x in Fig. 3a) and particulate matter (PM10 in Fig. 3b). This situation motivated a series of initiatives, including the project Brenner Low Emission Corridor (BrennerLEC) and a recent study aimed at disentangling the impact of weather conditions on observed pollutant concentrations (Falocchi et al. 2021).

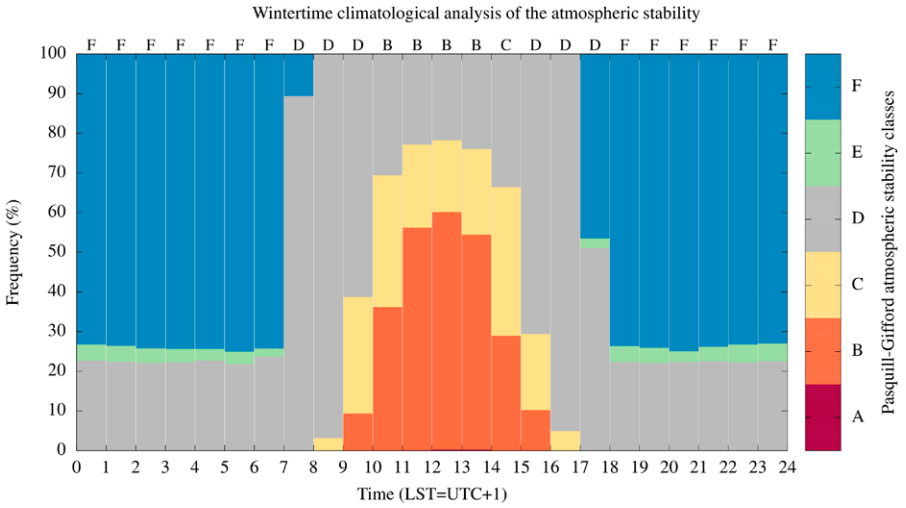

Fig. 2. Relative frequency of wintertime stability situations over the daily cycle in the Bolzano basin, based on Pasquill–Gifford stability classes, evaluated over the period December 2006–December 2014.

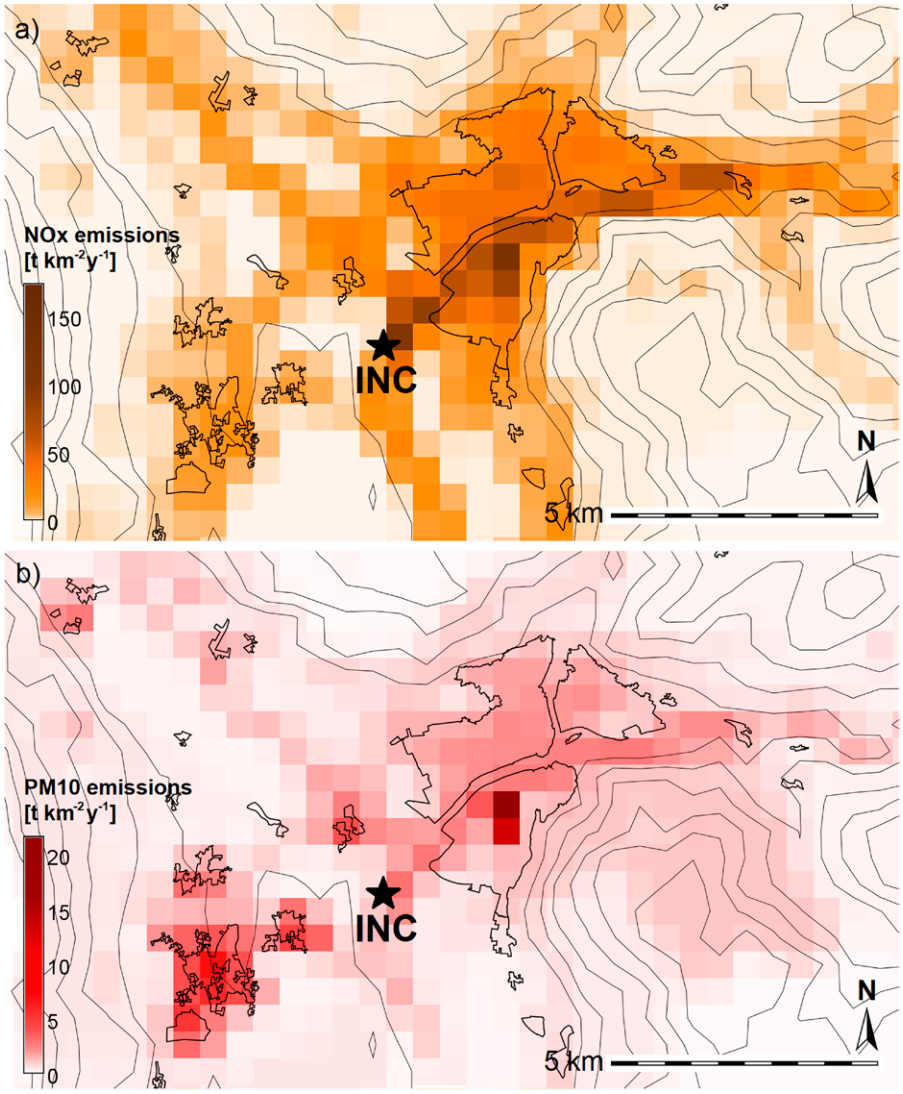

Fig. 3. Maps of mean annual surface emissions in the area surrounding Bolzano based on the Emission Inventory by the Environmental Protection Agency of the Autonomous Province of Bolzano: (a) NO_x and (b) particulate matter (PM10). The black star indicates the incinerator.

Valley exit jets

Valley exit jets are a peculiar case of nocturnal down-valley winds occurring at the exit of a narrow valley on a wider adjacent area, such as a plain, or a basin, or a wider valley (Zardi and Whiteman 2013). According to Chrust et al. (2013), valley exit jets can develop as thermally driven flows when the synoptic forcing is weak and the wind dynamics is only controlled by the temperature contrast between the air masses in the valley and outside its outlet. Conversely, dynamically driven valley exit jets may occur when mesoscale effects allow the penetration of synoptic winds into the valley, thus enforcing the local circulations. In either case, as a consequence of the cross-section widening, the cross-flow structure of the wind may expand (Fig. SB1). Instead, the modification of vertical structure on the lower layers is strongly dependent of the existing stratification in the wider area receiving the flow: low-level inversions often impede the downward penetration of momentum. As a result, the upper flow remains quite decoupled form the stable cold pool below.

A remarkable example of such a jet occurs at the outlet of the Inn Valley (Austria) onto the Bavarian Plain (Germany). Pamperin and Stilke (1985) provided observational evidences, later confirmed by numerically modeling simulation (Zängl 2004, 2008). More recently, Jiménez et al. (2019) performed mesoscale numerical simulations to investigate the formation of a valley exit jet at the mouth of the Aura Valley, in the Pyrenees, under different synoptic forcing.

Jet-like flows were also detected at the exit of tributary canyons from the Wasatch Mountains into the Salt Lake Valley (Banta et al. 1995, 2004; Fast and Darby 2004; Darby and Banta 2006; Darby et al. 2006).

Similar features occur on canyon-like valleys opening onto the plains south of Boulder, Colorado (Coulter and Gudiksen 1995; Doran 1996; Varvayanni et al. 1997), and at the exit of valleys issuing onto the Snake River plain in eastern Idaho (Stewart et al. 2002).

Valley exit jets may have a relevant impact on the boundary layer structures downstream to the valley exit (cf. Jiménez et al. 2019), as well as on the environment. For instance, when they advect cleaner air, they may have a cleansing effect in more polluted areas. Although they may be not so effective in removing pollutants for lower layers, as long as their stability prevents penetration, they can help wash out pollutants emitted from elevated sources (cf. Darby et al. 2006).

A similar situation has been more recently investigated in the Weber Canyon by Chrust et al. (2013).

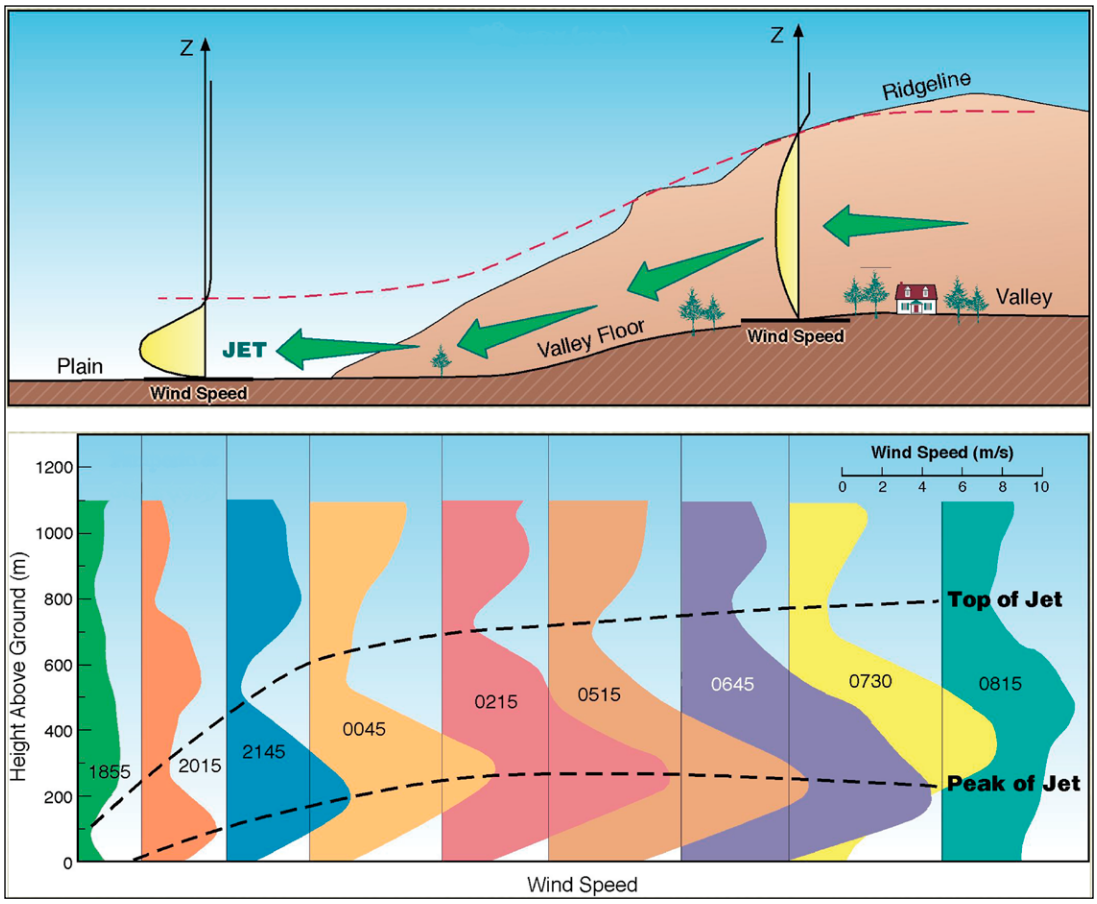

Fig. SB1. Schematic of a valley exit jet (reproduced with permission from Whiteman 2000).

Most of the pollutant-producing processes in the area—house heating, urban and extra-urban traffic, biomass burning, steel production, and waste treatment—involve combustion processes. Hence, the production of nitrogen oxides, as well as of both coarse and fine particulate matter, is more or less common to all of them. Consequently, none of these air pollutants could be unambiguously identified as a source-specific marker. It may be argued that species like polychlorinated biphenyl (PCB) and furans are usually listed among the typical emissions form waste incinerators (Ragazzi et al. 2013). However, these emissions are quite common also to other waste treatment processes existing in the area.

The complex situation described above, and the need for a reliable assessment of the impact of emissions from the sole incinerator, suggested to undertake a targeted investigation. Therefore, it was decided to perform an experiment including the release of a passive tracer from its chimney, based on previous examples from similar projects reported in Table 1.

Outline of the project and design of the experiment

Field monitoring system. Weather conditions over the whole target area were monitored throughout the experiment by means of a dense observational network including 15 permanent surface weather stations, one microwave temperature profiler, one sodar, and one Doppler wind lidar (Fig. 1).

The surface weather stations are operated by the Meteorological Service of the Autonomous Province of Bolzano. They are partly located on the valley floor, and partly on the sidewalls. These stations record 10-min air temperature and humidity at 2 m AGL, average wind intensity and direction and wind gusts at 10 m AGL, rainfall, atmospheric pressure, global solar radiation, and sunshine duration.

The atmospheric thermal structure inside the basin was constantly monitored by means of an MTP-5HE passive microwave radiometer (manufactured by Attex, Russia) installed at the airport of Bolzano, and routinely operated by the Environmental Protection Agency of the Autonomous Province of Bolzano. This device provides 10-min vertical temperature profiles from 10 to 1,000 m AGL (Falocchi et al. 2020).

The wind field at the chimney of the incinerator was monitored by means of a mini-sodar (MFAS Scintec, Germany) installed on the roof of the plant at 40 m AGL. The sodar probed the wind field from 55 to 425 m AGL with a vertical resolution of 30 m. Sodar measurements played a key role in the BTEX project. Indeed, the analysis of preliminary measurements in preparation for the experiment first allowed capturing a recurrent, intense nocturnal wind directed from the northeast, later identified as the valley exit jet from the Isarco Valley. As this airflow was expected to affect the dispersion of pollutants emitted from the incinerator, a targeted series of measurements was then specifically planned to monitor the jet structure and development. In particular, a Doppler wind lidar (WindCUBE 100S, Leosphere, France: label 4 in Fig. 1) was installed, from 9 January to 5 April 2017, on the roof of a building at 18 m AGL, in front of the Isarco Valley outlet (Fig. 4). Vertical wind profiles were measured every 18 s by means of a Doppler beam swinging (DBS) technique along 110 vertical levels, 10 m spaced, and with a vertical resolution of 25 m.

Weather situation. The experiment was performed on 14 February 2017, in the absence of significant synoptic forcing. Two tracer releases were performed, at two different day times, to explore different stability and wind direction conditions. The first release was planned in the early morning (0700 LST), with a stably stratified atmosphere and weak down-valley wind, and the second in the early afternoon (1245 LST), with weakly unstable atmosphere and up-valley wind. Indeed, synoptic conditions were dominated by a strong high pressure system, extending over most of central Europe, leading to weak southerly winds over northern Italy (Fig. 5). This situation allowed the development of typical thermally driven circulations in the

Fig. 4. Vacuum-filled bottles installed at selected sampling points during the experiments, with the waste incinerator in the background: (a) northward view from sampling point 9 in Fig. 7b, (b) southward view from sampling point 10 in Fig. 7b.

valleys surrounding the Bolzano basin, characterized by weak down- and up-valley winds in the Adige Valley during nighttime and daytime, respectively, and by a stronger down-valley flow in the Isarco Valley, generating the valley exit jet described in the "Outline of the situation" section, as can be seen in Fig. 6. During the night between 13 and 14 February low-level clouds reduced radiative cooling, resulting in a night warmer than the previous one, and preventing the development of a ground-based inversion. The Isarco Valley exit jet was clearly detected by the Doppler lidar after 2100 LST (UTC + 1), becoming stronger and deeper until early morning (0900 LST 14 February), when it reached its maximum intensity, above 13 m s^{-1}. Shortly after, it ceased quite abruptly around 1100 LST, as is typical of these phenomena (Banta et al. 1995; Chrust et al. 2013). After 1200 LST 14 February, both the sodar and the Doppler wind lidar observed a weak up-valley wind in the Adige Valley, as detected by surface weather stations as well.

Setup and execution of the tracer experiment. The ideal tracer for the investigation of atmospheric dispersion processes needs to meet a series of requirements, which actually reduce the choice to a relatively restricted range of chemical compounds (Johnson 1983; Martin et al. 2011). First, it should be practically absent from the ambient air, as well as easily measurable in the laboratory from samples collected

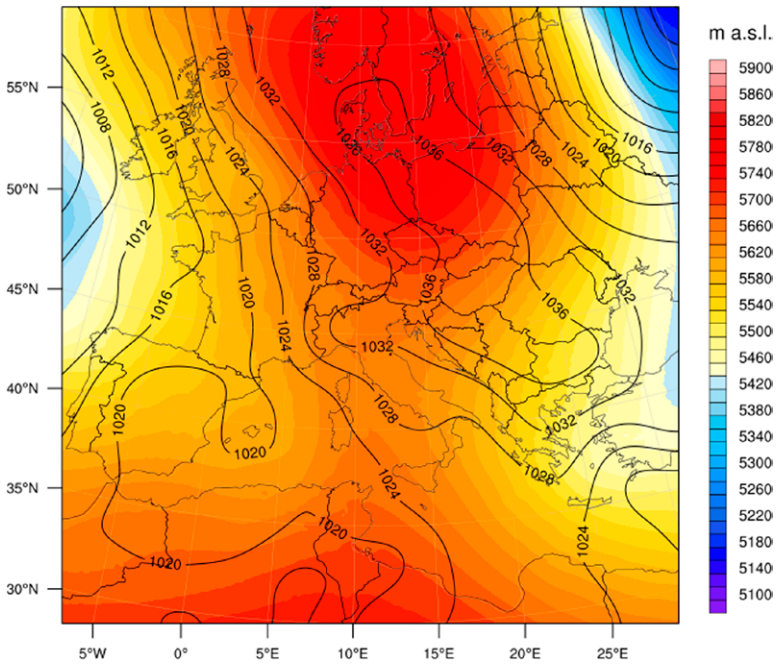

Fig. 5. Weather situation on 17 Feb 2017 right before the time of the first release of the tracer: solid lines are isobars at the mean sea level surface, and the color scale is the geopotential height of the 500-hPa isosurface.

in the field. Also, for environmental reasons, it has to be colorless and odorless, as well as not harmful for either the human health or the environment. Finally, it has to be chemically inert and stable, even at the high temperature of the smoke where it is injected. Sulfur hexafluoride (SF_6) turned out to be a good candidate. SF_6 does not exist in nature and is produced industrially, mostly for applications in electric devices as an insulator. The most important source likely to alter the background concentration are leakages from industrial plants. However, its background at planetary level is reported to be about 10 pptv (cf. Rigby et al. 2010; Manca 2017). For these reasons, it has been widely used in many studies of pollutant dispersion from industrial plants in different regions, including mountain valleys and urban environments.

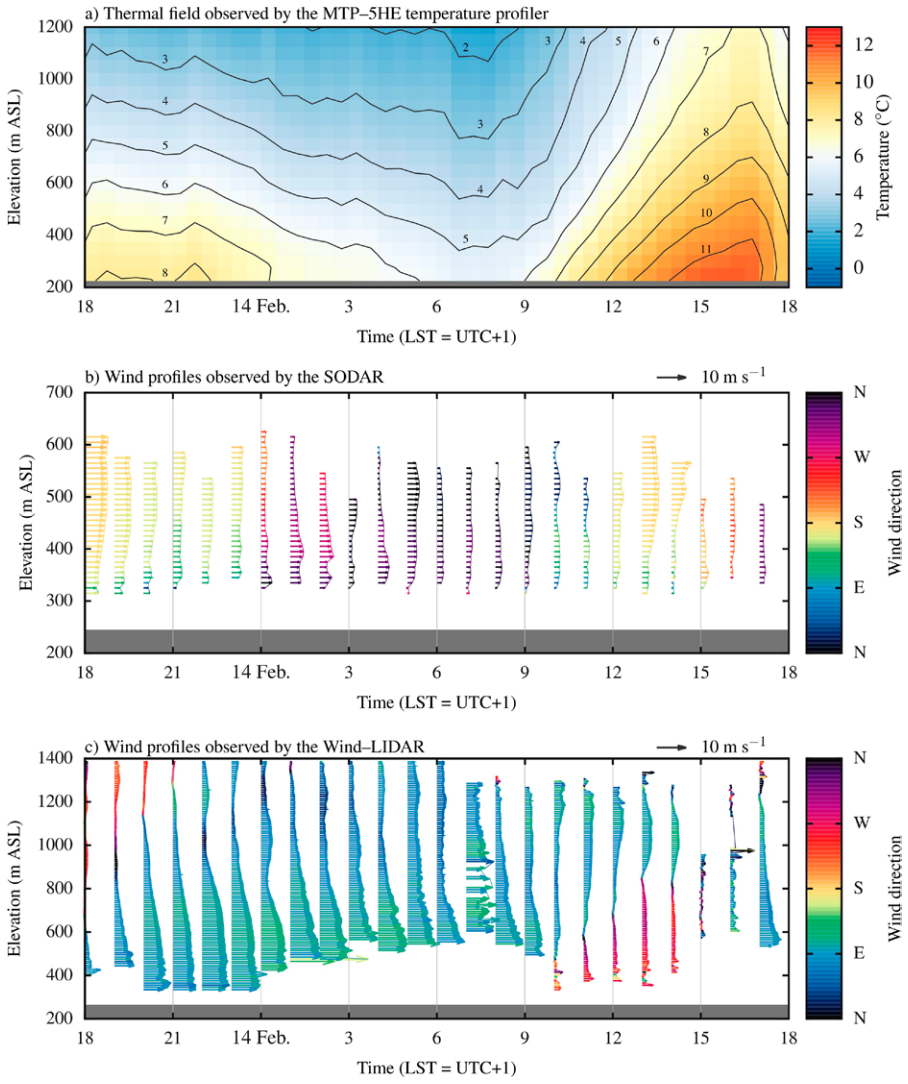

Fig. 6. Evolution of the vertical structure of the atmosphere in the Bolzano basin during the tracer experiment. (a) Vertical temperature profiles from the MTP5 based at the airport, and vertical profiles of (b) wind direction and (c) wind strength from the sodar installed on the incinerator roof.

Since many industrial activities are based in Bolzano and surroundings, a preliminary campaign was performed to investigate the background SF_6 concentration in the ambient air prior to any release. Concentrations were found to be lower than 30 pptv, i.e., well in the order of magnitude of the global background concentration (Rigby et al. 2010).

In view of producing a continuous and consistent cloud of tracer out of the stack, it was of utmost importance to release SF_6 at a constant rate into the steady flow of the smoke, as well as to ensure a good mixing throughout the chimney pipe cross section before emission into the atmosphere. Therefore, SF_6 was injected at the bottom of the stack, upstream of the ventilation system, to guarantee an effective mixing of the tracer within the smoke. Suitable regulation of the outflow from the tank containing the tracer allowed a precise control on the mass flow rate. As a further check, an online mass spectrometer was added to the existing online smoke-monitoring system to monitor the actual SF_6 concentration before emission into the atmosphere. A summary of timing, duration, mass of tracer injected, and emission characteristics, as well as samples collected for the two releases, is shown in Table 2.

Fourteen teams of personnel equipped with vacuum-filled glass bottles and plastic (PVF) bags were arranged in the envisaged ground-level impact area, to collect samples of ambient air. Bottles with a capacity of 1 L were filled by means of valves with calibrated nozzles,

Table 2. Summary of the two releases performed during BTEX (VB: vacuum-filled glass bottles, PB: PVF bags).

Release				Plant smoke		Samples		
No.	Start	Duration (min)	Tracer mass (kg)	Temperature (°C)	Exit speed (m s^{-1})	Points	VB	PB
1	0700 LST	60	150	140	7.9	14	25	3
2	1245 LST	90	450	140	7.8	14	30	21

allowing a constant inflow. Plastic bags were inflated by means of suitable pumps. Sampling-point positions, as well as nozzle-opening times and durations, were decided on the basis of targeted weather and dispersion forecasts. The optimal layout of the samplers required some reasoning. Indeed, the nontrivial orography did not allow for simple geometrical layouts, such as concentric circles around the source, or other "regular" patterns downstream of the source. Therefore, a numerical modeling chain was specifically set up to provide the best estimate of the surface impact area. The chain was optimized for fast runs, based on last-minute input from the weather monitoring network, in view of guiding fine-tuning adjustments of the samplers' positions.

Seven sampling teams were located close to the main residential areas—where most of the environmental receptors are concentrated—while the other ones were placed in the surroundings of the incinerator, especially in the most likely impact areas, according to the modeling results. The collected samples of ambient air were later analyzed in the laboratory by means of a triple quadrupole gas chromatography mass spectrometer. Results from the concentration measurements are represented in Fig. 7. Figure 7a shows the time evolution of the concentrations measured during each release: each line represents one sampling point (SP), identified by its reference number (left column). These lines are placed on the ordinate according to their latitude (from south to north), for easier comparison with the maps in Figs. 7b and 7c. The horizontal black lines mark the latitude of the incinerator, for reference.

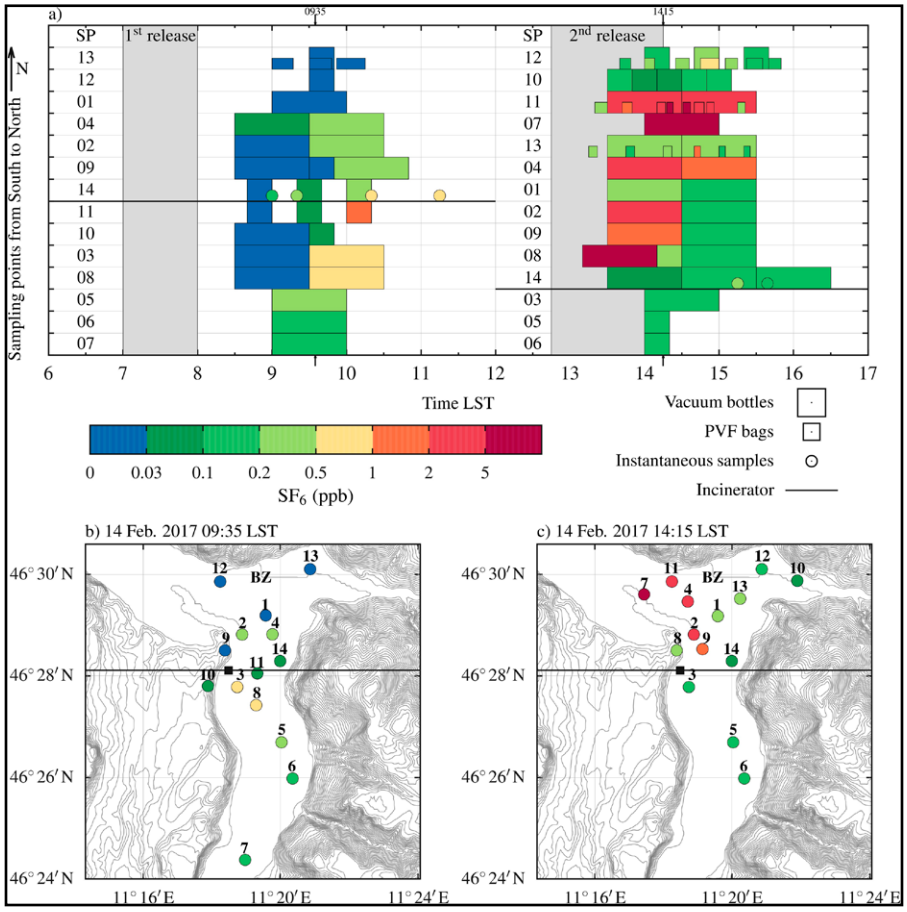

Fig. 7. (a) Time history of SF_6 concentration measured after each release, according to the color scale. The gray bands indicates the timing and duration of each release. Large colored rectangles: air samples collected by vacuum-filled glass bottles. Small rectangles: air samples collected by PVF bags. Circles: instant samples. (b),(c) Distribution of sampling points in the target area for the first and second release, respectively: bullets indicate sampling points, and colors refer to the average tracer concentration measured at the point. Horizontal black lines indicate the latitude of the incinerator, whose position is marked by a black square in (b) and (c).

The first release was carried out in the early morning, i.e., in a stable nocturnal atmosphere with a light down-valley wind. The valley exit jet from the Isarco Valley was confined north of the incinerator and did not interact with the smokes. Forecasts of such atmospheric conditions led to envisage a weak dispersion of the tracer and an impact area south of the incinerator. The tracer release started at 0700 LST and ended 1 h later, whereas the sampling activity started at 0830 LST and continued until 1045 LST. At the beginning of the sampling period, only one team northeast of the incinerator observed a concentration of SF_6 significantly different from the background (0.03–0.1 ppb), whereas at 0915 LST the tracer was clearly detected south of the incinerator in the Adige Valley, with concentrations ranging between 0.1 and 0.5 ppb. These findings confirm that the transport of the tracer due to the advection by the mean wind (of about 2–3 m s^{-1} above the incinerator, as shown by the sodar profiles in Fig. 6b) dominated over turbulent dispersion, and therefore the impact of the tracer at surface level was lower and deferred. After 0930 LST the solar heating of the ground and the following onset of a weak up-valley wind (of about 2–4 m s^{-1} above the incinerator: see again Fig. 6b) promoted higher concentrations in the surrounding area north to it. However, coherent with the observed wind speed and direction, the tracer never really reached the city of Bolzano.

The second release started at 1245 LST and ended at 1415 LST, under a weakly unstable atmosphere and an up-valley wind rising in the Adige Valley. Expecting a stronger mixing, and hence a faster surface impact closer to the incinerator, samples were collected starting from 1310 LST (i.e., with the release still ongoing) until 1630 LST. Indeed, a concentration of 11.96 ppb was observed north of the incinerator at 1315 LST, i.e., already 30 min after the beginning of the release. At the end of the release (1415 LST), the up-valley wind moved the smokes of the plant northward, and significant concentrations of SF_6 were measured west of Bolzano, inside the basin, while trace concentrations were also observed south of the incinerator. After 30 min, the tracer spread into the basin, even if high concentrations were still observed west of Bolzano. Background concentrations of SF_6, ranging between 0.2 and 0.5 ppb, were also detected, very likely residuals from the morning release. At the end of the second release a total of 51 samples were collected by means of both vacuum-filled glass bottles and plastic bags.

Modeling

Real-time forecasting chain. In view of optimizing the location of the sampling teams, as soon as possible after each injection of the tracer, the dispersion process was simulated by means of a real-time modeling chain, including a numerical weather prediction model (WRF) and two different dispersion models (CALPUFF and SPRAY-WEB). WRF runs were performed on four nested domains: the inner domain covered an area of approximately 20 km^2 in the basin, with a horizontal resolution of 500 m. Simulations were initialized with the most recent available runs from the Global Forecast System (GFS), with a horizontal resolution of 0.25°. Data assimilation was performed by means of observational nudging of all the available measurements. To simulate the fate of the tracer, WRF was coupled with two different dispersion models: the CALPUFF semi-Lagrangian Gaussian puff model (Scire et al. 2000), and the SPRAY-WEB particle Lagrangian model (Tinarelli et al. 1994, 2000; Alessandrini et al. 2005; Alessandrini and Ferrero 2009; Bisignano et al. 2017, 2019). CALPUFF simulations were run with a horizontal spatial resolution of 200 m, adopting the diagnostic model CALMET as meteorological preprocessor. As to the simulations with SPRAY-WEB, a WRF–SPRAY-WEB interface was specifically developed to process and feed WRF data into SPRAY-WEB (Tomasi et al. 2017). Real-time results obtained from this modeling chain were useful as primary information for deciding the location of the sampling teams in the Bolzano basin, on the basis of the forecasted impact area of the tracer.

Ex-post simulations. After the experiment, a series of model runs were performed in view of testing against field measurements the performance of dispersion modeling chains similar to those set up for real-time forecasts, but run in ex-post mode. The meteorological fields were again calculated by means of the WRF Model. However, as computational time was not any more a limiting factor in the ex-post analysis, a refined simulation of phenomena was pursued. In particular, a finer horizontal and vertical grid spacing was adopted. Three two-way nested domains were used, with horizontal resolution of 4.5, 0.9, and 0.3 km, respectively, and a very fine vertical grid in the lowest atmospheric layers, resulting in a total of 62 vertical levels, with 10 levels in the first 300 m AGL, and other 14 levels between 300 m and 1 km AGL. Meteorological boundary and initial conditions were derived from 6-hourly ECMWF HRES Operational Data, with 9-km resolution. The simulation covered the release day of BTEX, running from 1200 UTC 13 February 2017 to 0000 UTC 15 February 2017, for a total of 36 h. The first 12 h were used to spin up the model, hence the corresponding results were not analyzed.

The physics schemes adopted were the WRF single-moment 3-class scheme for microphysics (Hong et al. 2004), the RRTMG scheme for long- and shortwave radiation (Iacono et al. 2008), the Noah land surface model (Chen and Dudhia 2001), and the 1.5-order Nakanishi and Niino (2004) scheme for PBL parameterization. The default set of closure constants was modified as suggested in Trini Castelli et al. (1999, 2001), on the basis of turbulence measurements over an idealized valley in a wind-tunnel experiment. Hourly observational nudging was performed in the innermost domain, and all the available meteorological observations described in the "Outline of the situation" section were assimilated.

Preliminary WRF simulations outlined that a straightforward application of input data from the global meteorological model led to an overestimation of the snow cover over most of the domain. The resulting unrealistic surface forcing led the model to simulate a stronger down-valley wind in the upper Adige Valley, with no resemblance with observations from the numerous weather stations in the area. A more realistic representation of meteorological quantities was obtained after modifying the snow cover as suggested in Tomasi et al. (2019).

Dispersion simulations with both models started at 0700 LST (first SF_6 release) and ended at 1800 LST (5 h after the second release). The emission from the chimney was represented as a prescribed steady flow from a point source at 60 m AGL (the height of the stack) with a constant concentration of tracer throughout the duration of each release. CALPUFF simulation (CP) was performed at 300 m horizontal resolution, with 10 vertical levels up to 3000 m (having the first level at 20 m AGL). Being that SPRAY-WEB is a Lagrangian model, neither horizontal nor vertical grids need to be prescribed. However, ground concentrations were returned on a grid with 300-m horizontal and 20-m vertical resolution.

For both dispersion models, meteorological data were derived from WRF output: for CALPUFF through the preprocessor CALMET, and for SPRAY-WEB through the WRF–SPRAY-WEB interface. In particular, CALMET extracts from WRF output the mean meteorological variables and recalculates the surface layer (SL) scales (such as friction velocity, convective velocity scale, Obukhov length, and mixing height) based on an internal micrometeorological parameterization. These SL scales are then used to calculate standard deviations of wind velocities by means of a formulation combining different empirical relations and theoretical results from Panofsky et al. (1977), Hicks (1985), Arya (1984), Blackadar and Tennekes (1968), Nieuwstadt (1984), and Hanna et al. (1986). Such a formulation allows a consistent evaluation of the standard deviations and their vertical structures across convective, neutral, and stable stratification, without any physically unrealistic discontinuity. Instead, the WRF–SPRAY-WEB interface directly extracts from WRF output all the required meteorological variables, including SL scales and turbulence quantities. Therefore, for the calculation of the wind standard deviations, different methods can be adopted, depending on the choice of variables to be derived from WRF output. In particular, for the present analysis, three

different SPRAY-WEB simulations were performed, using three distinct methods for calculating standard deviations on the basis of different input from WRF, namely,

(i) SPRAY-WEB with the Hanna (1982) parameterization (hereafter labeled SPWH), using SL scales from WRF;
(ii) SPRAY-WEB with the previously cited CALPUFF inner parameterization (SPWC), using SL scales from WRF;
(iii) SPRAY-WEB with the TKE parameterization, using turbulence information from the WRF planetary boundary layer scheme (SPWTKE), as in Bisignano et al. (2017).

Both models implement suitable schemes for the estimate of the effective source height. In particular, in CALPUFF the plume rise is calculated from Briggs (1975) formulae, whereas SPRAY-WEB adopts the formulation by Anfossi (1985), which is a generalization of Briggs (1975), implemented as described in Anfossi et al. (1993). The effective source heights calculated by the two models were closely similar for the morning release, about 110 m above the emission source (i.e., about 170 m AGL), whereas for the afternoon they spanned between 90 and 150 m above the emission point (i.e., 150 and 210 m AGL).

Discussion of results

Results from the experiments provided an observational basis to compare, in a particularly challenging situation, the performance of the Gaussian-puff model CALPUFF, widely used for regulatory purposes, against a Lagrangian particle model, SPRAY-WEB, generally adopted for research applications only. All the models received as an input the same meteorological fields produced by WRF simulations. SPRAY-WEB was run with three different schemes for calculating wind velocity variances (SPWC, SPWH, SPWTKE), as explained above, to test their performance. Indeed, one of the most significant sources of uncertainty in meteorological dispersion modeling chains is the calculation of quantities required to simulate turbulent diffusion processes. These are usually obtained from a meteorological model output through a meteorological preprocessor (Colonna et al. 2009; Ferrero and Colonna 2006; Ferrero et al. 2018, 2003; Trini Castelli et al. 1999, 2001; Ferrero and Racca 2004). However, this procedure may be particularly critical over complex terrain, where the applicability of scaling laws implemented in the models—mostly based on Monin–Obukhov similarity theory for flat uniform terrain—is not granted (cf. Giovannini et al. 2020).

We will concentrate here on tracer concentration fields as reproduced by dispersion models' runs; for a more detailed analysis of the meteorological fields resulting from WRF simulations, the interested reader may refer to Tomasi et al. (2019).

Figures 8 and 9 show the different concentration distributions reproduced by the four dispersion simulations at two different time snapshots after each of the two releases, i.e., at 0900 and 1415 LST,

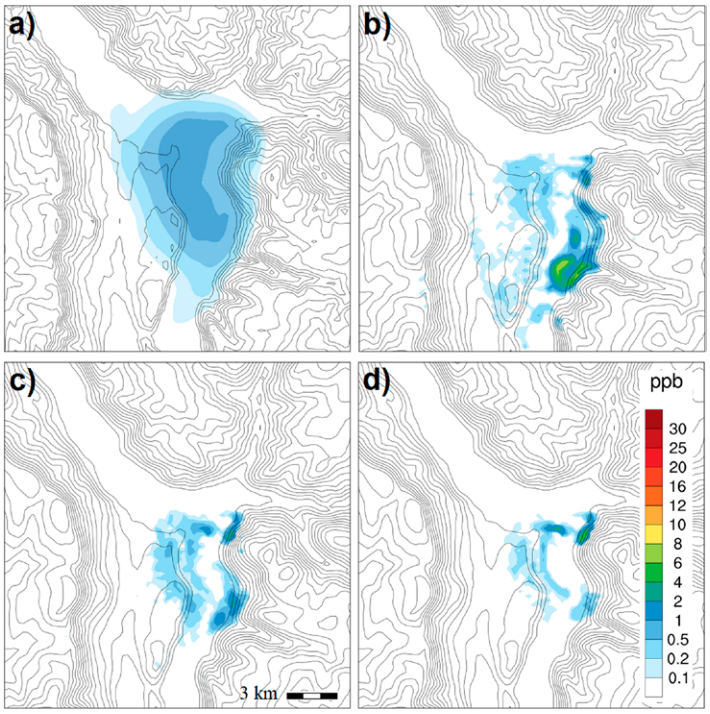

Fig. 8. Ground level concentration following the first release at 0900 LST simulated by (a) CP, (b) SPWC, (c) SPWH, and (d) SPWTKE.

respectively. A first qualitative analysis suggests that the tracer cloud is appropriately advected in the direction suggested by wind observations (i.e., down-valley in the morning, up-valley toward the city during the afternoon). However, the dispersion of the tracer is simulated quite differently by the models: CP produces quite uniform patterns, very insensitive to the surrounding complex topography and the associated wind field, whereas orographic features seem to significantly affect all ground concentrations simulated by SPRAY-WEB, generating more realistic dispersion scenarios. Comparing situations resulting from the morning and from the afternoon release, it is clearly seen how in the morning the weak vertical mixing, associated with stable stratification conditions, reduced the ground impact of the tracer. This is particularly evident in simulations from SPWTKE. Also notice the models' disagreement in localizing ground concentration maxima—quite apart from the source, anyway. Instead, for the afternoon release, when weakly unstable conditions promoted a more significant vertical mixing of the northward-advected cloud, models substantially agree in locating the maximum ground impact north of the incinerator, and quite close to it. However, to obtain a quantitative evaluation of the models' ability in reproducing ground tracer concentrations, suitable objective indexes were calculated (cf. Weil et al. 1992; Chang and Hanna 2004). In particular, the statistical indexes used here are the mean $\overline{M}$ of the N modeled values M_i ($i = 1, \ldots, N$), compared with the mean $\overline{O}$ of the observations O_i, the correlation R, the fractional bias FB, and the normalized mean square error NMSE, defined as follows:

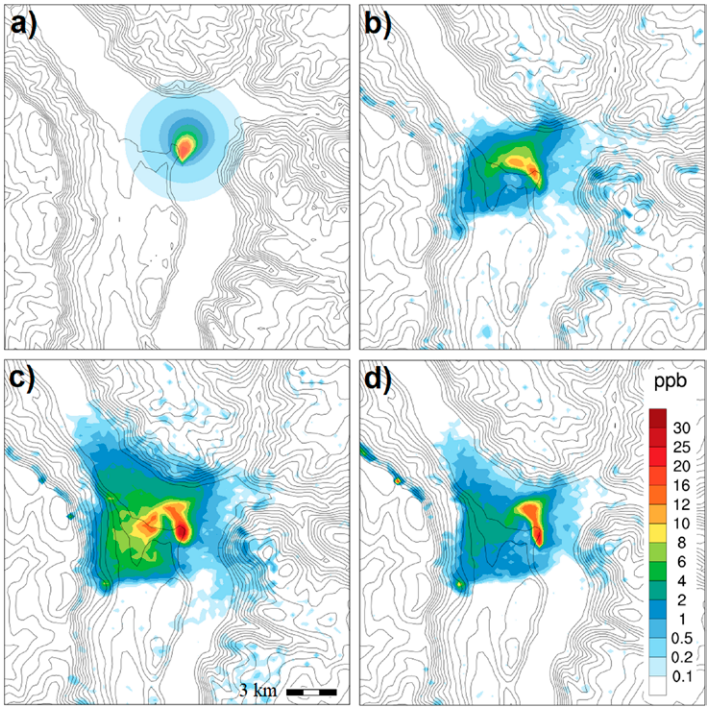

Fig. 9. Ground level concentration following the first release at 1415 LST simulated by (a) CP, (b) SPWC, (c) SPWH, and (d) SPWTKE.

$$R = \frac{\sum_{i=1}^{N}\left(O_i - \overline{O}\right)\left(M_i - \overline{M}\right)}{\sqrt{\sum_{i=1}^{N}\left(O_i - \overline{O}\right)^2}\sqrt{\sum_{i=1}^{N}\left(M_i - \overline{M}\right)^2}}, \tag{1}$$

$$\mathrm{FB} = 2\frac{\overline{O} - \overline{M}}{\overline{O} + \overline{M}}, \tag{2}$$

$$\mathrm{NMSE} = N\frac{\sum_{i=1}^{N}\left(M_i - O_i\right)^2}{\sum_{i=1}^{N} M_i \sum_{i=1}^{N} O_i}. \tag{3}$$

Values of the above indexes, calculated for all model runs, are shown in Table 3: all in all, CP presents the worst performance, with a consistent overestimation and no appreciable correlation with observations, whereas SPWTKE displays the best evaluation statistics for all the indexes. A good performance, similar to SPWTKE, is displayed also by SPWC, while SPWH

significantly overestimates the observed ground concentrations.

Similar considerations can be drawn from results presented in Figs. 10 and 11, showing observed and modeled concentration quantiles, in terms of percentile distribution and Q–Q plots, respectively, for each simulation. Comparison of the graphics confirms that both CP and SPWH systematically tend to overestimate tracer concentrations. However, CP presents the largest errors mostly at low percentiles, while SPWH at concentration peaks. SPWC has a similar behavior to SPWH up to the 85th percentile, but with a slight underestimation of the concentrations at higher percentiles. This suggests that the low fractional bias displayed by this simulation results from the compensation of overestimations at low percentiles and underestimations at high percentiles. Again, it is quite evident that the best results are achieved by SPWTKE, which well captures both low concentrations and peak values, the only significant discrepancy occurring for the 90th percentile value, which is appreciably underestimated.

Table 3. Statistical indexes calculated for each simulation: $\bar{O}$ is the mean of observations, $\bar{M}$ is the mean of the modeled values, R is the correlation, FB the fractional bias, and NMSE is the normalized mean square error (see text for the corresponding formulas). The best values of the indexes are in bold.

Simulation	$\bar{O}$ (pptv)	$\bar{M}$ (pptv)	R	FB	NMSE
CP	900	1,298	0.05	0.36	6.64
SPWC		980	0.70	0.09	2.43
SPWH		1,266	0.68	0.34	3.82
SPWTKE		**888**	**0.76**	**−0.01**	**2.23**

Conclusions

The Bolzano Tracer Experiment (BTEX) offered an unprecedented opportunity to investigate boundary layer processes and local airflows in the basin surrounding the city of Bolzano in the Alps. A remarkable concentration of observing systems allowed characterizing typical wintertime situations in the basin in much detail. Data from SF_6 concentration measurements following two releases of the tracer through the chimney of the incinerator provided a valuable basis for testing and comparing the performance of different numerical model chains for weather and pollutant dispersion prediction.

As expected, the CALPUFF Gaussian puff model performs much worse compared to the SPRAY-WEB Lagrangian model. Mean concentration values are greatly overestimated, as the emitted puffs essentially hit the ground uniformly.

Results obtained from BTEX show that the combination of a meteorological model, including appropriate turbulence closures for complex terrain, and a dispersion simulation run with a turbulence parameterization based on TKE can lead to a better reconstruction of the dispersion parameters. In turn, better values of dispersion parameters result in a better prediction of ground-level concentrations. These results confirm that closures specifically calibrated for complex terrain are of utmost importance for improving the numerical simulation of dispersion processes in mountainous areas (Giovannini et al. 2020). Further improvements may be obtained by including suitable parameterizations appropriate for

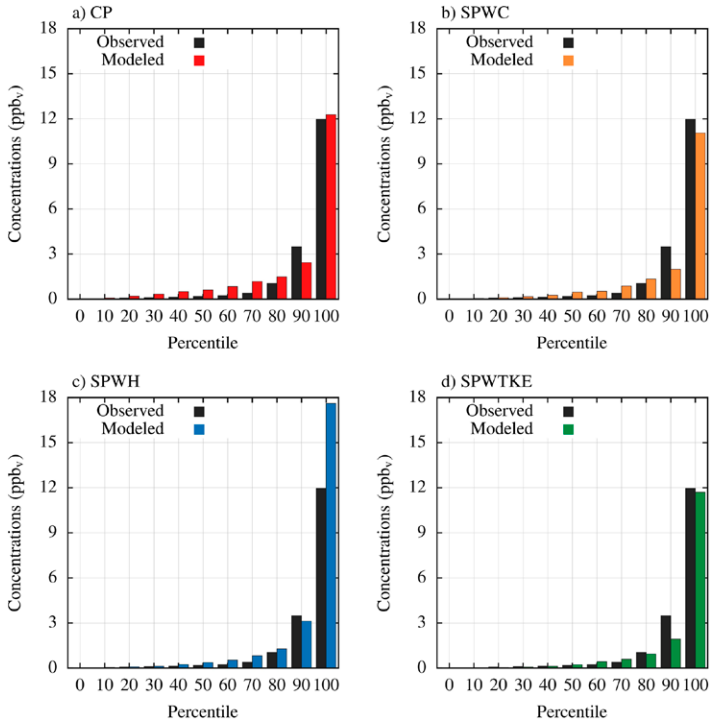

Fig. 10. Percentile curves of observed ground concentrations against model output values from simulations (a) CP, (b) SPWC, (c) SPWH, and (d) SPWTKE. Bar colors match corresponding cases in Fig. 11.

the different scales of turbulence, where deviations from isotropy, associated with terrain complexity, may significantly affect diffusion processes (Falocchi et al. 2019; Stiperski et al. 2019).

However, it should be recognized that the above results suffer from the limitation of being conducted with only two releases. The differences between the SPWC and SPWTKE simulations (Table 3) are quite small, especially in view of the large NMSE. A much larger number of releases, observations, and model results would be needed to tease out small statistical differences, given the large scatter.

Furthermore, the present analysis focuses on near-surface concentrations only, as during the experiment only ground measurements were collected. This is indeed a limitation of the analysis, as the vertical transport is an important feature in evaluating boundary layer schemes. Future investigations are therefore needed to draw conclusions on the performance of the different schemes in capturing the dispersion along the vertical direction. Ongoing research programs, which aim at updating surface layer theories and scaling laws, to account for terrain complexity and horizontal nonhomogeneity (cf. Serafin et al. 2018) are therefore expected to cast new light for our understanding of the above processes and to provide better tools for modeling them. The dataset from BTEX—which is available for public download, as indicated in Falocchi et al. (2020)—will provide a benchmark for evaluation of these models too.

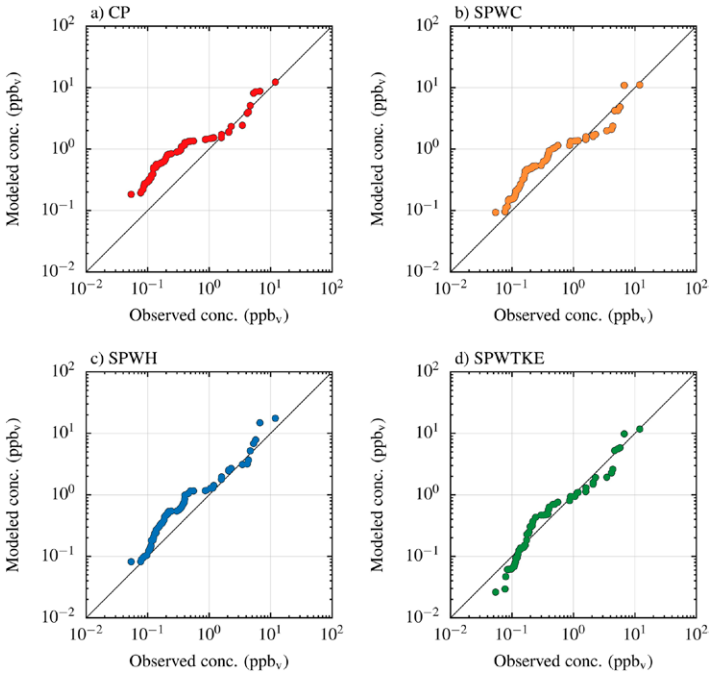

Fig. 11. Q–Q plots of the observed ground concentrations and corresponding values modeled from simulations with (a) CP, (b) SPWC, (c) SPWH, and (d) SPWTKE.

Acknowledgments. We would like to acknowledge high performance computing support from Cheyenne (doi:10.5065/D6RX99HX) provided by NCAR's Computational and Information Systems Laboratory, sponsored by the National Science Foundation.

The authors acknowledge Eco-Center s.p.a. for the financial support to the project, and in particular Marco Palmitano and Bruno Eisenstecken, who encouraged and supervised the project throughout its development. The authors are also grateful to all the personnel of Eco-Center s.p.a., Eco-Research s.r.l., the Environmental Agency of the Autonomous Province of Bolzano and the "Mario Negri Institute" for participating in the measurement activities during the releases. The Meteorological Office of the Autonomous Province of Bolzano is acknowledged for kindly providing data from their weather stations. The Environmental Agency of the Autonomous Province of Bolzano, Massimo Guariento, and Dr. Luca Verdi are kindly acknowledged for data from the microwave temperature profiler and from the Emission Inventory.

References

Alessandrini, S., and E. Ferrero, 2009: A hybrid Lagrangian-Eulerian particle model for reacting pollutant dispersion in non-homogeneous non- isotropic turbulence. *Physica A*, **388**, 1375–1387, https://doi.org/10.1016/j.physa.2008.12.015.

——, ——, C. Pertot, and E. Orlandi, 2005: Comparison of different dispersion models with tracer experiment. *Nuovo Cimento*, **28**, 141–149, https://doi.org/10.1393/NCC/I2005-10187-0.

Allwine, K. J., 1993: Atmospheric dispersion and tracer ventilation in a deep mountain valley. *J. Appl. Meteor.*, **32**, 1017–1037, https://doi.org/10.1175/1520-0450(1993)032<1017:ADATVI>2.0.CO;2.

——, and J. E. Flaherty, 2006: Joint Urban 2003: Study overview and instrument locations. Rep. PNNL-15967, 92 pp., www.pnnl.gov/main/publications/external/technical_reports/PNNL-15967.pdf.

——, B. K. Lamb, and R. Eskridge, 1992: Wintertime dispersion in a mountainous basin at Roanoke, Virginia: Tracer study. *J. Appl. Meteor.*, **31**, 1295–1311, https://doi.org/10.1175/1520-0450(1992)031<1295:WDIAMB>2.0.CO;2.

——, J. H. Shinn, G. E. Streit, K. L. Clawson, and M. Brown, 2002: Overview of URBAN 2000. *Bull. Amer. Meteor. Soc.*, **83**, 521–536, https://doi.org/10.1175/1520-0477(2002)083<0521:OOUAMF>2.3.CO;2.

——, M. Leach, L. Stockham, J. Shinn, R. Hosker, J. Bowers, and J. Pace, 2004: Overview of Joint Urban 2003: An atmospheric dispersion study in Oklahoma City. *Symp. on Planning, Nowcasting and Forecasting in the Urban Zone* and *Eighth Symp. on Integrated Observing and Assimilation Systems for Atmosphere, Oceans, and Land Surface*, Seattle, WA. Amer. Meteor. Soc., J7.1, https://ams.confex.com/ams/84Annual/techprogram/paper_74349.htm.

Ambrosetti, P., D. Anfossi, S. Cieslik, G. Graziani, G. Grippa, R. L. A. Marzorati, A. Stingele, and H. Zimmermann, 1994: The TRANSALP-90 Campaign: The second tracer release experiment in a sub-alpine valley. Tech. Rep. EUR 15952 EN, 70 pp., https://op.europa.eu/en/publication-detail/-/publication/3c1e5150-ef36-443c-8fbd-4a3e7067087b.

——, and Coauthors, 1998: Mesoscale transport of atmospheric trace constituents across the central Alps: Transalp tracer experiments. *Atmos. Environ.*, **32**, 1257–1272, https://doi.org/10.1016/S1352-2310(97)00185-4.

Anfossi, D., 1985: Analysis of plume rise data from five TVA Steam Plants. *J. Climate Appl. Meteor.*, **24**, 1225–1236, https://doi.org/10.1175/1520-0450(1985)024<1225:AOPRDF>2.0.CO;2.

——, E. Ferrero, G. Brusasca, A. Marzorati, and G. Tinarelli, 1993: A simple way of computing buoyant plume rise in Lagrangian stochastic dispersion models. *Atmos. Environ.*, **27**, 1443–1451, https://doi.org/10.1016/0960-1686(93)90130-Q.

Arduini, G., C. Staquet, and C. Chemel, 2016: Interactions between the night-time valley-wind system and a developing cold-air pool. *Bound.-Layer Meteor.*, **161**, 49–72, https://doi.org/10.1007/s10546-016-0155-8.

——, C. Chemel, and C. Staquet, 2020: Local and non-local controls on a persistent cold-air pool in the Arve River Valley. *Quart. J. Roy. Meteor. Soc.*, **146**, 2497–2521, https://doi.org/10.1002/qj.3776.

Arya, S., 1984: Parametric relations for the atmospheric boundary layer. *Bound.-Layer Meteor.*, **30**, 57–73, https://doi.org/10.1007/BF00121949.

Banta, R. M., L. D. Olivier, W. N. Neff, D. H. Levinson, and D. Ruffieux, 1995: Influence of canyon-induced flows on flow and dispersion over adjacent plains. *Theor. Appl. Climatol.*, **52**, 27–42, https://doi.org/10.1007/BF00865505.

——, L. S. Darby, J. D. Fast, J. Pinto, C. D. Whiteman, W. J. Shaw, and B. D. Orr, 2004: Nocturnal low-level jet in a mountain basin complex. I: Evolution and effects on local flows. *J. Appl. Meteor.*, **43**, 1348–1365, https://doi.org/10.1175/JAM2142.1.

Barad, M. L., Ed., 1958: Project prairie grass, A field program in diffusion. Geophysical Research Papers, No. 59, Vols. I and II, Air Force Cambridge Research Center Rep. AFCRC-TR-58-235, 479 pp.

Bisignano, A., L. Mortarini, E. Ferrero, and S. Alessandrini, 2017: Model chain for buoyant plume dispersion. *Int. J. Environ. Pollut.*, **62**, 200–213, https://doi.org/10.1504/IJEP.2017.089406.

——, E. Ferrero, and S. Alessandrini, 2019: A Lagrangian dispersion model with a stochastic equation for the temperature fluctuations. *Int. J. Environ. Pollut.*, **65**, 311–324, https://doi.org/10.1504/IJEP.2019.103747.

Blackadar, A., and H. Tennekes, 1968: Asymptotic similarity in neutral barotropic planetary boundary layers. *J. Atmos. Sci.*, **25**, 1015–1020, https://doi.org/10.1175/1520-0469(1968)025<1015:ASINBP>2.0.CO;2.

Bowen, B. M., 1994: Long-term tracer study at Los Alamos, New Mexico. Part I: Wind, turbulence, and tracer patterns. *J. Appl. Meteor.*, **33**, 1221–1235, https://doi.org/10.1175/1520-0450(1994)033<1221:LTTSAL>2.0.CO;2.

Bowne, N. E., R. J. Londergan, D. R. Murray, and H. S. Borenstein, 1983: Overview, results, and conclusions for the EPRI Plume Model Validation and Development Project: Plains site. Electric Power Research Institute Rep. EA-3074, 230 pp.

Briggs, G. A., 1975: Plume rise predictions. *Lectures on Air Pollution and Environmental Impact Analysis*, Amer. Meteor. Soc., 59–111.

Britter, R. E., S. Di Sabatino, F. Caton, K. M. Cooke, P. G. Simmonds, and G. Nickless, 2002: Results from three field tracer experiments on the neighbourhood scale in the City of Birmingham UK. *Water Air Soil Pollut. Focus*, **2**, 79–90, https://doi.org/10.1023/A:1021306612036.

Bruintjes, R. T., T. L. Clark, and W. D. Hall, 1995: The dispersion of tracer plumes in mountainous regions in Central Arizona: Comparisons between observations and modeling results. *J. Appl. Meteor.*, **34**, 971–988, https://doi.org/10.1175/1520-0450(1995)034<0971:TDOTPI>2.0.CO;2.

Chang, J. C., and S. R. Hanna, 2004: Air quality model performance evaluation. *Meteor. Atmos. Phys.*, **87**, 167–196, https://doi.org/10.1007/s00703-003-0070-7.

Chen, F., and J. Dudhia, 2001: Coupling an advanced land surface-hydrology model with the Penn State–NCAR MM5 modeling system. Part I: Model implementation and sensitivity. *Mon. Wea. Rev.*, **129**, 569–585, https://doi.org/10.1175/1520-0493(2001)129<0569:CAALSH>2.0.CO;2.

Chen, J., R. Bornstein, and C. G. Lindsey, 1999: Transport of a power plant tracer plume over Grand Canyon National Park. *J. Appl. Meteor.*, **38**, 1049–1068, https://doi.org/10.1175/1520-0450(1999)038<1049:TOAPPT>2.0.CO;2.

Chrust, M., C. Whiteman, and S. Hoch, 2013: Observations of thermally driven wind jets at the exit of Weber Canyon, Utah. *J. Appl. Meteor. Climatol.*, **52**, 1187–1200, https://doi.org/10.1175/JAMC-D-12-0221.1.

Clawson, K. L., and Coauthors, 2005: Joint Urban 2003 (JU03) SF6 atmospheric tracer field tests. NOAA Tech. Memo. OAR ARL-254, Air Resources Laboratory, 237 pp.

Clements, W. E., J. A. Archuleta, and P. H. Gudiksen, 1989: Experimental design of the 1984 ASCOT field study. *J. Appl. Meteor.*, **28**, 405–413, https://doi.org/10.1175/1520-0450(1989)028<0405:EDOTAF>2.0.CO;2.

Colonna, N., E. Ferrero, and U. Rizza, 2009: Nonlocal boundary layer: The pure buoyancy driven and the buoyancy-shear-driven cases. *J. Geophys. Res.*, **114**, D05102, https://doi.org/10.1029/2008JD010682.

Conangla, L., J. Cuxart, M. A. Jiménez, D. Martínez-Villagrasa, J. R. Miró, D. Tabarelli, and D. Zardi, 2018: Cold-air pool evolution in a wide Pyrenean valley. *Int. J. Climatol.*, **38**, 2852–2865, https://doi.org/10.1002/joc.5467.

Connan, O., P. Laguionie, D. Maro, D. Hébert, P. Mestayer, F. Rodriguez, V. Rodrigues, and J. Rosant, 2015: Vertical and horizontal concentration profiles from a tracer experiment in a heterogeneous urban area. *Atmos. Res.*, **154**, 126–137, https://doi.org/10.1016/j.atmosres.2014.11.009.

Coulter, R. L., and P. Gudiksen, 1995: The dependence of canyon winds on surface cooling and external forcing in Colorado's Front Range. *J. Appl. Meteor.*, **34**, 1419–1429, https://doi.org/10.1175/1520-0450(1995)034<1419:TDOCWO>2.0.CO;2.

Cramer, H. E., F. A. Record, and H. C. Vaughan, 1958: The study of the diffusion of gases or aerosols in the lower atmosphere. Rep. AFCRC-TR-58-239, Department of Meteorology, Massachusetts Institute of Technology, 133 pp.

Darby, L. S., and R. M. Banta, 2006: The modulation of canyon flows by larger-scale influences. *12th Conf. Mountain Meteorology*, Santa Fe, NM, Amer. Meteor. Soc., 14.4, https://ams.confex.com/ams/SantaFe2006/techprogram/paper_114383.htm.

——, K. J. Allwine, and R. M. Banta, 2006: Nocturnal low-level jet in a mountain basin complex. Part II: Transport and diffusion of tracer under stable conditions. *J. Appl. Meteor. Climatol.*, **45**, 740–753, https://doi.org/10.1175/JAM2367.1.

de Franceschi, M., and D. Zardi, 2009: Study of wintertime high pollution episodes during the Brenner-South ALPNAP measurement campaign. *Meteor. Atmos. Phys.*, **103**, 237–250, https://doi.org/10.1007/s00703-008-0327-2.

——, ——, M. Tagliazucca, and F. Tampieri, 2009: Analysis of second order moments in the surface layer turbulence in an Alpine valley. *Quart. J. Roy. Meteor. Soc.*, **135**, 1750–1765, https://doi.org/10.1002/qj.506.

De Wekker, S. F. J., M. Kossmann, J. C. Knievel, L. Giovannini, E. D. Gutmann, and D. Zardi, 2018: Meteorological applications benefiting from an improved understanding of atmospheric exchange processes over mountains. *Atmosphere*, **9**, 371, https://doi.org/10.3390/atmos9100371.

Dickerson, M. H., and P. H. Gudiksen, 1983: Atmospheric studies in complex terrain. Tech. Progress Rep. FY 1979–FY 1983, 367 pp.

Doran, J. C., 1996: The influence of canyon winds on flow fields near Colorado's Front Range. *J. Appl. Meteor.*, **35**, 587–600, https://doi.org/10.1175/1520-0450(1996)035<0587:TIOCWO>2.0.CO;2.

——, and T. W. Horst, 1985: An evaluation of Gaussian plume-depletion models with dual-tracer field measurements. *Atmos. Environ.*, **19**, 939–951, https://doi.org/10.1016/0004-6981(85)90239-2.

——, J. D. Fast, and J. Horel, 2002: The VTMX 2000 campaign. *Bull. Amer. Meteor. Soc.*, **83**, 537–551, https://doi.org/10.1175/1520-0477(2002)083<0537:TVC>2.3.CO;2.

——, K. J. Allwine, J. E. Flaherty, K. L. Clawson, and R. G. Carter, 2007: Characteristics of puff dispersion in an urban environment. *Atmos. Environ.*, **41**, 3440–3452, https://doi.org/10.1016/j.atmosenv.2006.12.029.

Dosio, A., S. Emeis, G. Graziani, W. Junkermann, and A. Levy, 2001: Assessing the meteorological conditions of a deep Italian Alpine valley system by means of a measuring campaign and simulations with two models during a summer smog episode. *Atmos. Environ.*, **35**, 5441–5454, https://doi.org/10.1016/S1352-2310(01)00285-0.

Draxler, R., 1985: Metropolitan Tracer Experiment (METREX). NOAA Tech. Memo. ERL ARL-140, 85, 102 pp.

——, and J. L. Heffter, Eds., 1989: Across North America Tracer Experiment (ANATEX) Volume I: Description, ground-level sampling at primary sites, and meteorology. NOAA Tech. Memo. ERL ARL-167, 83 pp., www.arl.noaa.gov/documents/reports/arl-167.pdf.

Eastman, J. L., R. A. Pielke, and W. A. Lyons, 1995: Comparison of lake-breeze model simulations with tracer data. *J. Appl. Meteor.*, **34**, 1398–1418, https://doi.org/10.1175/1520-0450(1995)034<1398:COLBMS>2.0.CO;2.

Emberlin, J. C., 1981: A sulphur hexafluoride tracer experiment from a tall stack over complex topography in a coastal area of Southern England. *Atmos. Environ.*, **15**, 1523–1530, https://doi.org/10.1016/0004-6981(81)90134-7.

Falocchi, M., L. Giovannini, M. de Franceschi, and D. Zardi, 2019: A method to determine the characteristic time scales of quasi-isotropic surface-layer turbulence over complex terrain: A case-study in the Adige Valley (Italian Alps). *Quart. J. Roy. Meteor. Soc.*, **145**, 495–512, https://doi.org/10.1002/qj.3444.

——, W. Tirler, L. Giovannini, E. Tomasi, G. Antonacci, and D. Zardi, 2020: A dataset of tracer concentrations and meteorological observations from the Bolzano Tracer EXperiment (BTEX) to characterize pollutant dispersion processes in an Alpine valley. *Earth Syst. Sci. Data*, **12**, 277–291, https://doi.org/10.5194/essd-12-277-2020.

——, D. Zardi, and L. Giovannini, 2021: Meteorological normalization of NO_2 concentrations in the Province of Bolzano (Italian Alps). *Atmos. Environ.*, **246**, 118048, https://doi.org/10.1016/j.atmosenv.2020.118048.

Fast, J. D., and L. S. Darby, 2004: An evaluation of mesoscale model predictions of down-valley and canyon flows and their consequences using Doppler lidar measurements during VTMX 2000. *J. Appl. Meteor.*, **43**, 420–436, https://doi.org/10.1175/1520-0450(2004)043<0420:AEOMMP>2.0.CO;2.

——, K. J. Allwine, R. N. Dietz, K. L. Clawson, and J. C. Torcolini, 2006: Dispersion of perfluorocarbon tracers within the Salt Lake Valley during VTMX 2000. *J. Appl. Meteor. Climatol.*, **45**, 793–812, https://doi.org/10.1175/JAM2371.1.

Ferber, G. J., K. Telegadas, J. L. Heffter, C. R. Dickson, R. N. Dietz, and P. W. Krey, 1981: Demonstration of a long-range atmospheric tracer system using perfluorocarbons. NOAA Tech. Memo. ERL ARL-101, 74 pp.

——, and Coauthors, 1986: Cross-Appalachian tracer experiment (CAPTEX '83) final report. NOAA Tech. Memo. ERL ARL-142, 60 pp.

Fernando, H. J., and Coauthors, 2015: The MATERHORN: Unraveling the intricacies of mountain weather. *Bull. Amer. Meteor. Soc.*, **96**, 1945–1967, https://doi.org/10.1175/BAMS-D-13-00131.1.

Ferrero, E., and N. Colonna, 2006: Nonlocal treatment of the buoyancy-shear-driven boundary layer. *J. Atmos. Sci.*, **63**, 2653–2662, https://doi.org/10.1175/JAS3789.1.

——, and M. Racca, 2004: The role of the non-local transport in modelling the shear-driven atmospheric boundary layer. *J. Atmos. Sci.*, **61**, 1434–1445, https://doi.org/10.1175/1520-0469(2004)061<1434:TROTNT>2.0.CO;2.

——, S. Trini Castelli, and D. Anfossi, 2003: Turbulence fields for atmospheric dispersion models in horizontally non-homogeneous conditions. *Atmos. Environ.*, **37**, 2305–2315, https://doi.org/10.1016/S1352-2310(03)00179-1.

——, S. Alessandrini, and F. Vandenberghe, 2018: Assessment of planetary-boundary layer schemes in the weather research and forecasting model within and above an urban canopy layer. *Bound.-Layer Meteor.*, **168**, 289–319, https://doi.org/10.1007/s10546-018-0349-3.

Fiedler, F., I. Bischoff-Gauß, N. Kalthoff, and G. Adrian, 2000: Modeling of the transport and diffusion of a tracer in the Freiburg-Schauinsland area. *J. Geophys. Res.*, **105**, 1599–1610, https://doi.org/10.1029/1999JD900911.

Flaherty, J. E., B. Lamb, K. J. Allwine, and E. Allwine, 2007: Vertical tracer concentration profiles measured during the joint urban 2003 dispersion study. *J. Appl. Meteor. Climatol.*, **46**, 2019–2037, https://doi.org/10.1175/2006JAMC1305.1.

Flesch, T. K., J. D. Wilson, L. A. Harper, B. P. Crenna, and R. R. Sharpe, 2004: Deducing ground-to-air emissions from observed trace gas concentrations: A field trial. *J. Appl. Meteor.*, **43**, 487–502, https://doi.org/10.1175/1520-0450(2004)043<0487:DGEFOT>2.0.CO;2.

Fuquay, J. J., C. L. Simpson, and W. T. Hinds, 1964: Prediction of environmental exposures from sources near the ground based on Hanford experimental data. *J. Appl. Meteor.*, **3**, 761–770, https://doi.org/10.1175/1520-0450(1964)003<0761:POEEFS>2.0.CO;2.

Giovannini, L., G. Antonacci, D. Zardi, L. Laiti, and L. Panziera, 2014a: Sensitivity of simulated wind speed to spatial resolution over complex terrain. *Energy Procedia*, **59**, 323–329, https://doi.org/10.1016/j.egypro.2014.10.384.

——, D. Zardi, M. de Franceschi, and F. Chen, 2014b: Numerical simulations of boundary-layer processes and urban-induced alterations in an Alpine valley. *Int. J. Climatol.*, **34**, 1111–1131, https://doi.org/10.1002/joc.3750.

——, L. Laiti, D. Zardi, and M. de Franceschi, 2015: Climatological characteristics of the Ora del Garda wind in the Alps. *Int. J. Climatol.*, **35**, 4103–4115, https://doi.org/10.1002/joc.4270.

——, ——, S. Serafin, and D. Zardi, 2017: The thermally driven diurnal wind system of the Adige Valley in the Italian Alps. *Quart. J. Roy. Meteor. Soc.*, **143**, 2389–2402, https://doi.org/10.1002/qj.3092.

——, E. Ferrero, T. Karl, M. W. Rotach, C. Staquet, S. Trini Castelli, and D. Zardi, 2020: Atmospheric pollutant dispersion over complex terrain: Challenges and needs for improving air quality measurements and modelling. *Atmosphere*, **11**, 646, https://doi.org/10.3390/atmos11060646.

Gohm, A., and Coauthors, 2009: Air pollution transport in an alpine valley: Results from airborne and ground-based observations. *Bound.-Layer Meteor.*, **131**, 441–463, https://doi.org/10.1007/s10546-009-9371-9.

Green, M. C., 1999: The project MOHAVE tracer study: Study design, data quality, and overview of results. *Atmos. Environ.*, **33**, 1955–1968, https://doi.org/10.1016/S1352-2310(98)00126-5.

Gryning, S. E., and E. Lyck, 1980: Elevated source SF6-tracer dispersion experiments in the Copenhagen area: Preliminary results II. *Proc. Seminar on Radioactive Releases and their Dispersion in the Atmosphere Following a Hypothetical Reactor Accident*, Roskilde, Denmark, Commission of the European Communities, 905–924.

——, ——, 1984: Atmospheric dispersion from elevated sources in an urban area: Comparison between tracer experiments and model calculations. *J.*

Climate Appl. Meteor., **23**, 651–660, https://doi.org/10.1175/1520-0450(1984)023<0651:ADFESI>2.0.CO;2.

——, ——, 2002: The Copenhagen tracer experiments: Reporting of measurements. Risø-R-1054(rev.1)(EN), Riso National Laboratory, 75 pp., http://orbit.dtu.dk/files/7726795/ris_r_1054_rev1.pdf.

Gudiksen, P. H., and D. L. Shearer, 1989: The dispersion of atmospheric tracers in nocturnal drainage flows. *J. Appl. Meteor.*, **28**, 602–608, https://doi.org/10.1175/1520-0450(1989)028<0602:TDOATI>2.0.CO;2.

Haagenson, P. L., Y. Kuo, M. Syumanich, and N. L. Seaman, 1987: Tracer verification of trajectory models. *J. Climate Appl. Meteor.*, **26**, 410–426, https://doi.org/10.1175/1520-0450(1987)026<0410:TVOTM>2.0.CO;2.

——, K. Gao, and Y. Kuo, 1990: Evaluation of meteorological analyses, simulations, and long-range transport calculations using ANATEX surface tracer data. *J. Appl. Meteor.*, **29**, 1268–1283, https://doi.org/10.1175/1520-0450(1990)029<1268:EOMASA>2.0.CO;2.

Hanna, S. R., 1982: Applications in Air Pollution Modeling. *Atmospheric Turbulence and Air Pollution Modelling: A Course Held in The Hague, 21–25 September 1981*, F. T. M. Nieuwstadt and H. van Dop, Eds., Springer, 275–310.

——, B. A. Egan, C. J. Vaudo, and A. J. Curreri, 1984: A complex terrain dispersion model for regulatory applications at the Westvaco Luke Mill. *Atmos. Environ.*, **18**, 685–699, https://doi.org/10.1016/0004-6981(84)90255-5.

——, J. Weil, and R. Paine, 1986: Plume model development and evaluation. Tech. Rep. D034-500, Electric Power Research Institute, 550 pp.

Haugen, D. A., Ed., 1959: Project Prairie Grass, a field program in diffusion. Vol. III, Geophysical Research Papers 59, Air Force Cambridge Research Center Rep. AFCRC-TR-58-235, 673 pp., NTIS PB 161 101.

——, and J. J. Fuquay, Eds., 1963: The ocean breeze and dry gulch diffusion programs, Vol. I. Air Force Cambridge Research Laboratories and Hanford Atomic Products Operations Rep. HW-78435, 240 pp.

Heffter, J. L., J. F. Schubert, and G. A. Mead, 1984: Atlantic Coast Unique Regional Atmospheric Tracer Experiment (ACURATE). NOAA Tech. Memo. ERL ARL-130, 15 pp.

Hegarty, J., and Coauthors, 2013: Evaluation of Lagrangian particle dispersion models with measurements from controlled tracer releases. *J. Appl. Meteor. Climatol.*, **52**, 2623–2637, https://doi.org/10.1175/JAMC-D-13-0125.1.

Hicks, B. B., 1985: Behavior of turbulence statistics in the convective boundary layer. *J. Climate Appl. Meteor.*, **24**, 607–614, https://doi.org/10.1175/1520-0450(1985)024<0607:BOTSIT>2.0.CO;2.

Hong, S.-Y., J. Dudhia, and S.-H. Chen, 2004: A revised approach to ice microphysical processes for the bulk parameterization of clouds and precipitation. *Mon. Wea. Rev.*, **132**, 103–120, https://doi.org/10.1175/1520-0493(2004)132<0103:ARATIM>2.0.CO;2.

Iacono, M. J., J. S. Delamere, E. J. Mlawer, M. W. Shephard, S. A. Clough, and W. D. Collins, 2008: Radiative forcing by long-lived greenhouse gases: Calculations with the AER radiative transfer models. *J. Geophys. Res.*, **113**, D13103, https://doi.org/10.1029/2008JD009944.

Jiménez, M. A., J. Cuxart, and D. Martínez-Villagrasa, 2019: Influence of a valley exit jet on the nocturnal atmospheric boundary layer at the foothills of the Pyrenees. *Quart. J. Roy. Meteor. Soc.*, **145**, 356–375, https://doi.org/10.1002/qj.3437.

Johnson, W. B., 1983: Meteorological tracer techniques for parameterizing atmospheric dispersion. *J. Climate Appl. Meteor.*, **22**, 931–946, https://doi.org/10.1175/1520-0450(1983)022<0931:MTTFPA>2.0.CO;2.

Kalthoff, N., V. Horlacher, U. Corsmeier, A. Volz Thomas, B. Kolahgar, H. Geiß, M. Möllmann-Coers, and A. Knaps, 2000: Influence of valley winds on transport and dispersion of airborne pollutants in the Freiburg-Schauinsland area. *J. Geophys. Res.*, **105**, 1585–1597, https://doi.org/10.1029/1999JD900999.

Koračin, D., J. Frye, and V. Isakov, 2000: A method of evaluating atmospheric models using tracer measurements. *J. Appl. Meteor.*, **39**, 201–221, https://doi.org/10.1175/1520-0450(2000)039<0201:AMOEAM>2.0.CO;2.

Laiti, L., D. Zardi, M. de Franceschi, and G. Rampanelli, 2013a: Atmospheric boundary layer structures associated with the Ora del Garda wind in the Alps as revealed from airborne and surface measurements. *Atmos. Res.*, **132–133**, 473–489, https://doi.org/10.1016/j.atmosres.2013.07.006.

——, ——, ——, and ——, 2013b: Residual kriging analysis of airborne measurements: Application to the mapping of atmospheric boundary-layer thermal structures in a mountain valley. *Atmos. Sci. Lett.*, **14**, 79–85, https://doi.org/10.1002/asl2.420.

——, ——, G. Giovannini, M. de Franceschi, and G. Rampanelli, 2014: Analysis of the diurnal development of a lake-valley circulation in the Alps based on airborne and surface measurements. *Atmos. Chem. Phys.*, **14**, 9771–9786, https://doi.org/10.5194/acp-14-9771-2014.

——, L. Giovannini, D. Zardi, G. Belluardo, and D. Moser, 2018: Estimating hourly beam and diffuse solar radiation in an alpine valley: A critical assessment of decomposition models. *Atmosphere*, **9**, 117, https://doi.org/10.3390/atmos9040117.

Lareau, N. P., E. Crosman, C. D. Whiteman, J. Horel, S. Hoch, W. Brown, and T. W. Horst, 2013: The persistent cold-air pool study. *Bull. Amer. Meteor. Soc.*, **94**, 51–63, https://doi.org/10.1175/BAMS-D-11-00255.1.

Largeron, Y., and C. Staquet, 2016a: The atmospheric boundary layer during wintertime persistent inversions in the Grenoble valleys. *Front. Earth Sci.*, **4**, 70, https://doi.org/10.3389/feart.2016.00070.

——, and ——, 2016b: Persistent inversion dynamics and wintertime PM10 air pollution in Alpine valleys. *Atmos. Environ.*, **135**, 92–108, https://doi.org/10.1016/j.atmosenv.2016.03.045.

Manca, G., 2017: GreenHouse Gases concentration-2017. European Commission, Joint Research Centre (JRC), https://data.jrc.ec.europa.eu/dataset/jrc-abcis-ghg-2017.

Martin, D., and Coauthors, 2010a: Urban tracer dispersion experiment in London (DAPPLE) 2003: Field study and comparison with empirical prediction. *Atmos. Sci. Lett.*, **11**, 241–248, https://doi.org/10.1002/asl.282.

——, and Coauthors, 2010b: Urban tracer dispersion experiments during the second DAPPLE field campaign in London 2004. *Atmos. Environ.*, **44**, 3043–3052, https://doi.org/10.1016/j.atmosenv.2010.05.007.

——, K. F. Petersson, and D. E. Shallcross, 2011: The use of cyclic perfluoroalkanes and SF_6 in atmospheric dispersion experiments. *Quart. J. Roy. Meteor. Soc.*, **137**, 2047–2063, https://doi.org/10.1002/qj.881.

Mestayer, P. G., and Coauthors, 2011: Fluxsap 2010 experimental campaign over a heterogeneous urban zone, Part 1: heat and vapour flux assessment. *14th Int. Conf. on Harmonisation within Atmospheric Dispersion Modelling for Regulatory Purposes* , Kos Island, Greece, CCSD, 433–437.

Min, I. A., and Coauthors, 2002: Measurement and analysis of puff dispersion above the atmospheric boundary layer using quantitative imagery. *J. Appl. Meteor.*, **41**, 1027–1041, https://doi.org/10.1175/1520-0450(2002)041<1027:MAAOPD>2.0.CO;2.

Moran, M. D., and R. A. Pielke, 1996a: Evaluation of a mesoscale atmospheric dispersion modeling system with observations from the 1980 Great Plains mesoscale tracer field experiment. Part I: Datasets and meteorological simulations. *J. Appl. Meteor.*, **35**, 281–307, https://doi.org/10.1175/1520-0450(1996)035<0281:EOAMAD>2.0.CO;2.

——, and ——, 1996b: Evaluation of a mesoscale atmospheric dispersion modeling system with observations from the 1980 Great Plains mesoscale tracer field experiment. Part II: Dispersion simulations. *J. Appl. Meteor.*, **35**, 308–329, https://doi.org/10.1175/1520-0450(1996)035<0308:EOAMAD>2.0.CO;2.

Murray, D. R., and N. E. Bowne, 1988: Urban power plant plume studies. EPRI Rep. EA-5468, Research Project 2736-1, Electric Power Research Institute, 40 pp.

Nakanishi, M., and H. Niino, 2004: An improved Mellor–Yamada level-3 model with condensation physics: Its design and verification. *Bound.-Layer Meteor.*, **112**, 1–31, https://doi.org/10.1023/B:BOUN.0000020164.04146.98.

Ngan, F., and A. F. Stein, 2017: A long-term WRF meteorological archive for dispersion simulations: Application to controlled tracer experiments. *J. Appl. Meteor. Climatol.*, **56**, 2203–2220, https://doi.org/10.1175/JAMC-D-16-0345.1.

Ngan, F., A. Stein, and R. Draxler, 2015: Inline coupling of WRF–HYSPLIT: Model development and evaluation using tracer experiments. *J. Appl. Meteor. Climatol.*, **54**, 1162–1176, https://doi.org/10.1175/JAMC-D-14-0247.1.

Nickola, P. W., 1977: The Hanford 67-series: A volume of atmospheric field diffusion measurements. Rep. PNL-2433, Battelle Pacific Northwest Laboratories, 454 pp., https://doi.org/10.2172/5215934.

Nickola, P. W., J. V. Ramsdell, C. S. Glantz, and R. E. Kerns, 1983: Hanford atmospheric dispersion data: 1960 through June 1967. Rep. NUREG/CR-3456, PNL-4814, Battelle Pacific Northwest Laboratories, 683 pp., https://doi.org/10.2172/5360676.

Nieuwstadt, F., 1984: Some aspects of the turbulent stable boundary layer. *Bound.-Layer Meteor.*, **30**, 31–55, https://doi.org/10.1007/BF00121948.

Nieuwstadt, F. T. M., and H. van Duuren, 1979: Dispersion experiments with SF6 from the 213 m high meteorological mast at Cabauw in the Netherlands. *Proc. Fourth Symp. on Turbulence, Diffusion and Air Pollution*, Reno, Nevada, Amer. Meteor. Soc., 34–40.

Nodop, K., R. Connolly, and F. Girardi, 1998: The field campaigns of the European Tracer Experiment (ETEX): Overview and results. *Atmos. Environ.*, **32**, 4095–4108, https://doi.org/10.1016/S1352-2310(98)00190-3.

Orgill, M. M., 1989: Early morning ventilation of a gaseous tracer from a mountain valley. *J. Appl. Meteor.*, **28**, 636–651, https://doi.org/10.1175/1520-0450(1989)028<0636:EMVOAG>2.0.CO;2.

Paci, A., and Coauthors, 2016: La campagne Passy-2015: Dynamique atmosphérique et qualité de l'air dans la vallée de l'Arve [The Passy-2015 field experiment: Atmospheric dynamics and air quality in the Arve River Valley]. *Pollution atmosphérique*, **231–232**, https://doi.org/10.4267/pollution-atmospherique.5903.

Pamperin, H., and G. Stilke, 1985: Nächtliche Grenzschicht und LLJ im Alpenvorland nahe dem Inntalausgang [Nocturnal boundary layer and low level jet near the Inn Valley exit]. *Meteor. Rundsch.*, **38**, 145–156.

Panofsky, H., H. Tennekes, D. Lenschow, and J. Wyngaard, 1977: The characteristics of turbulent velocity components in the surface layer under convective conditions. *Bound.-Layer Meteor.*, **11**, 355–361, https://doi.org/10.1007/BF02186086.

Pennell, W. T., R. N. Lee, J. M. Hubbe, R. M. Enlich, M. A. Baugh, K. C. Nitz and W. B. Johnson, 1987: SCCCAMP Mesoscale Tracer Studies. Final Rep. SRI Proj. 8655, SCCCAMP Contract 126.53-18-SRI, SRI International, 115 pp

Pitchford, M., M. C. Green, and R. J. Farber, 1997: Characterization of regional transport and dispersion using Project MOHAVE tracer data. *Proc. Visual Air Quality: Aerosols and Global Radiation Balance*, Bartlett, NH, Air and Waste Management Association, 181–200.

Quimbayo-Duarte, J. A., C. Staquet, C. Chemel, and A. Arduini, 2019a: Impact of along-valley orographic variations on the dispersion of passive tracers in a stable atmosphere. *Atmosphere*, **10**, 225, https://doi.org/10.3390/atmos10040225.

Quimbayo-Duarte, J. A., C. Staquet, C. Chemel, and A. Arduini, 2019b: Dispersion of tracers in the stable atmosphere of a valley opening on a plain. *Bound.-Layer Meteor.*, **172**, 291–315, https://doi.org/10.1007/s10546-019-00439-2.

Ragazzi, M., W. Tirler, G. Angelucci, D. Zardi, and E. C. Rada, 2013: Management of atmospheric pollutants from waste incineration processes: The case of Bozen. *Waste Manage. Res.*, **31**, 235–240, https://doi.org/10.1177/0734242X12472707.

Rigby, M., and Coauthors, 2010: History of atmospheric SF_6 from 1973 to 2008. *Atmos. Chem. Phys.*, **10**, 10305–10320, https://doi.org/10.5194/acp-10-10305-2010.

Rotach, M. W., and D. Zardi, 2007: On the boundary–layer structure over highly complex terrain: Key findings from MAP. *Quart. J. Roy. Meteor. Soc.*, **133**, 937–948, https://doi.org/10.1002/qj.71.

——, and Coauthors, 2004a: Turbulence structure and exchange processes in an alpine valley: The Riviera Project. *Bull. Amer. Meteor. Soc.*, **85**, 1367–1386, https://doi.org/10.1175/BAMS-85-9-1367.

——, S. E. Gryning, E. Batchvarova, A. Christen, and R. Vogt, 2004b: Pollutant dispersion close to an urban surface–The BUBBLE tracer experiment. *Meteor. Atmos. Phys.*, **87**, 39–56, https://doi.org/10.1007/s00703-003-0060-9.

Sabatier, T., A. Paci, C. Lac, G. Canut, Y. Largeron, and V. Masson, 2020a: Semi-idealized simulations of wintertime flows and pollutant transport in an Alpine valley: Origins of local circulations (Part I). *Quart. J. Roy. Meteor. Soc.*, **146**, 807–826, https://doi.org/10.1002/qj.3727.

Sabatier, T., and Coauthors, 2020b: Semi-idealized simulations of wintertime flows and pollutant transport in an alpine valley. Part II: Passive tracer tracking. *Quart. J. Roy. Meteor. Soc.*, **146**, 827–845, https://doi.org/10.1002/qj.3710.

Schicker, I., and P. Seibert, 2009: Simulation of the meteorological conditions during a winter smog episode in the Inn Valley. *Meteor. Atmos. Phys.*, **103**, 211–222, https://doi.org/10.1007/s00703-008-0346-z.

Scire, J., D. Strimaitis, and R. Yamartino, 2000: A user's guide for the CALPUFF Dispersion Model (version 5.0). Tech. Rep., Earth Tech, Inc., 521 pp.

Serafin, S., and Coauthors, 2018: Exchange processes in the atmospheric boundary layer over mountainous terrain. *Atmosphere*, **9**, 102, https://doi.org/10.3390/atmos9030102.

Serafin, S., and Coauthors, 2020: Multi-scale transport and exchange processes in the atmosphere over mountains: Programme and experiment. Innsbruck University Press, 44 pp., https://doi.org/10.15203/99106-003-1.

Sivertsen, B., 1988: Tracer experiments to estimate diffusive leakages and to verify dispersion models. *Environmental Meteorology*, Springer, 255–268.

Sivertsen, B., and J. S. Irwin, 1987: Data Summary of 1985 SF6 Tracer Experiments at Andorra (Teruel) Power Plant. Tech. Rep. NILU OR 49/85, Norwegian Institute for Air Research, 74 pp.

Sivertsen, B., and J. S. Irwin, 1996: Tracer gas experiment to verify the dispersion from a tall stack. *Proc. Ninth Joint Conf. on Applications of Air Pollution Meteorology with A&WMA*, Atlanta, GA, Amer. Meteor. Soc., 41–43.

Stewart, J. Q., C. D. Whiteman, W. J. Steenburgh, and X. Bian, 2002: A climatological study of thermally driven wind systems of the US Intermountain West. *Bull. Amer. Meteor. Soc.*, **83**, 699–708, https://doi.org/10.1175/1520-0477(2002)083<0699:ACSOTD>2.3.CO;2.

Stiperski, I., M. Calaf, and M. W. Rotach, 2019: Scaling, anisotropy, and complexity in near-surface atmospheric turbulence. *J. Geophys. Res. Atmos.*, **124**, 1428–1448, https://doi.org/10.1029/2018JD029383.

Strimaitis, D. G., G. E. Moore, and S. G. Douglas, 1991: Analysis of tracer data collected during the SCCCAMP 1985 intensive measurement periods. *J. Appl. Meteor.*, **30**, 674–706, https://doi.org/10.1175/1520-0450(1991)030<0674:AOTDCD>2.0.CO;2.

Sykes, R. I., S. F. Parker, D. S. Henn, and W. S. Lewellen, 1993: Numerical simulation of ANATEX tracer data using a turbulence closure model for long-range dispersion. *J. Appl. Meteor.*, **32**, 929–947, https://doi.org/10.1175/1520-0450(1993)032<0929:NSOATD>2.0.CO;2.

Telegadas, K., G. J. Ferber, and R. R. Draxler, 1980: Measured weekly twice-daily krypton-85 surface air concentrations within 150 km of the Savannah River Plant (March 1975 through September 1977): Final report. NOAA Tech. Memo. ERL ARL-80, 97 pp.

Tinarelli, G., and Coauthors, 1994: Lagrangian particle simulation of tracer dispersion in the lee of a schematic two dimensional hill. *J. Appl. Meteor.*, **33**, 744–756, https://doi.org/10.1175/1520-0450(1994)033<0744:LPSOTD>2.0.CO;2.

Tinarelli, G., D. Anfossi, S. Trini Castelli, M. Bider, and E. Ferrero, 2000: A new high performance version of the Lagrangian particle dispersion model spray, some case studies. *Air Pollution Modeling and Its Application XIII*, S.-E. Gryning and E. Batchvarova, Eds., Springer, 499–507.

Tomasi, E., L. Giovannini, D. Zardi, and M. de Franceschi, 2017: Optimization of Noah and Noah_MP WRF land surface schemes in snow-melting conditions over complex terrain. *Mon. Wea. Rev.*, **145**, 4727–4745, https://doi.org/10.1175/MWR-D-16-0408.1.

——, and Coauthors, 2019: Turbulence parameterizations for dispersion in sub-kilometer horizontally non-homogeneous flows. *Atmos. Res.*, **228**, 122–136, https://doi.org/10.1016/j.atmosres.2019.05.018.

Trini Castelli, S., E. Ferrero, D. Anfossi, and R. Ying, 1999: Comparison of turbulence closure models over a schematic valley in a neutral boundary layer. *Proc. 13th Symp. on Boundary Layers and Turbulence* , Dallas, TX, Amer. Meteor. Soc., 601–604.

——, ——, and ——, 2001: Turbulence closures in neutral boundary layer over complex terrain. *Bound.-Layer Meteor.*, **100**, 405–419, https://doi.org/10.1023/A:1019208518127.

——, G. Belfiore, D. Anfossi, E. Elampe, and M. Clemente, 2011: Modelling the meteorology and traffic pollutant dispersion in highly complex terrain: The ALPNAP alpine space project. *Int. J. Environ. Pollut.*, **44**, 235–243, https://doi.org/10.1504/IJEP.2011.038423.

Van dop, H., and Coauthors, 1998: ETEX: A European tracer experiment; observations, dispersion modelling and emergency response. *Atmos. Env.*, **32**, 4089–4094, https://doi.org/10.1016/S1352-2310(98)00248-9.

Varvayanni, M., J. G. Bartzis, N. Catsaros, P. Deligianni, and C. E. Elderkin, 1997: Simulation of nocturnal drainage flows enhanced by deep canyons: The Rocky Flats case. *J. Appl. Meteor.*, **36**, 775–791, https://doi.org/10.1175/1520-0450-36.6.775.

Weil, J. C., R. I. Sykes, and A. Venkatram, 1992: Evaluating air quality models: Review and outlook. *J. Appl. Meteor.*, **31**, 1121–1145, https://doi.org/10.1175/1520-0450(1992)031<1121:EAQMRA>2.0.CO;2.

Whiteman, C. D., 1989: Morning transition tracer experiments in a deep narrow valley. *J. Appl. Meteor.*, **28**, 626–635, https://doi.org/10.1175/1520-0450(1989)028<0626:MTTEIA>2.0.CO;2.

——, 2000: *Mountain Meteorology: Fundamentals and Applications*. Oxford University Press, 355 pp.

Wilkerson, G., 1991: SF_6 tracer studies of the Lake Michigan Ozone study 1991 summer field program. NAWC Rep. AQ 91-23, 186 pp.

Wood, C. R., and Coauthors, 2009: Dispersion experiments in central London: The 2007 DAPPLE project. *Bull. Amer. Meteor. Soc.*, **90**, 955–970, https://doi.org/10.1175/2009BAMS2638.1.

Zängl, G., 2004: A reexamination of the valley wind system in the Alpine Inn Valley with numerical simulations. *Meteor. Atmos. Phys.*, **87**, 241–256, https://doi.org/10.1007/s00703-003-0056-5.

——, 2008: The impact of weak synoptic forcing on the valley-wind circulation in the Alpine Inn Valley. *Meteor. Atmos. Phys.*, **105**, 37–53, https://doi.org/10.1007/s00703-009-0030-y.

Zardi, D., and C. D. Whiteman, 2013: Diurnal mountain wind systems. *Mountain Weather Research and Forecasting – Recent Progress and Current Challenges*, F. K. Chow et al., Eds., Springer, 35–119.

Zimmermann, H., 1995: Field phase report of the TRACT field measurement campaign. EUROTRAC International Scientific Secretariat, 205 pp., https://www.osti.gov/etdeweb/biblio/221702.